WATER RESOURCES RESEARCH, VOL. 48, W04521, doi:10.1029/2011WR011188, 2012

Potential drought stress in a Swiss mountain catchment—Ensemble forecasting of high mountain soil moisture reveals a drastic decrease, despite major uncertainties

Ole Rössler,[1,2] Bernd Diekkrüger,[2] and Jörg Löffler[2]

Received 22 July 2011; revised 3 February 2012; accepted 24 February 2012; published 19 April 2012.

[1] Climate change is expected to profoundly influence the hydrosphere of mountain ecosystems. The focus of current process-based research is centered on the reaction of glaciers and runoff to climate change; spatially explicit impacts on soil moisture remain widely neglected. We spatio-temporally analyzed the impact of the climate on soil moisture in a mesoscale high mountain catchment to facilitate the development of mitigation and adaptation strategies at the level of vegetation patterns. Two regional climate models were downscaled using three different approaches (statistical downscaling, delta change, and direct use) to drive a hydrological model (WaSiM-ETH) for reference and scenario period (1960–1990 and 2070–2100), resulting in an ensemble forecast of six members. For all ensembles members we found large changes in temperature, resulting in decreasing snow and ice storage and earlier runoff, but only small changes in evapotranspiration. The occurrence of downscaled dry spells was found to fluctuate greatly, causing soil moisture depletion and drought stress potential to show high variability in both space and time. In general, the choice of the downscaling approach had a stronger influence on the results than the applied regional climate model. All of the results indicate that summer soil moisture decreases, which leads to more frequent declines below a critical soil moisture level and an advanced evapotranspiration deficit. Forests up to an elevation of 1800 m a.s.l. are likely to be threatened the most, while alpine areas and most pastures remain nearly unaffected. Nevertheless, the ensemble variability was found to be extremely high and should be interpreted as a bandwidth of possible future drought stress situations.

Citation: Rössler, O., B. Diekkrüger, and J. Löffler (2012), Potential drought stress in a Swiss mountain catchment—Ensemble forecasting of high mountain soil moisture reveals a drastic decrease, despite major uncertainties, *Water Resour. Res.*, *48*, W04521, doi:10.1029/2011WR011188.

1. Introduction and Aims

[2] With the ever-increasing certainty of global warming, sound climate change impact assessment studies are needed to facilitate the establishment of reasonable adaptation and mitigation strategies. For the European Alps, the *IPCC* [2007] and the PRUDENCE ensemble project [*Christensen et al.*, 2002] estimate an increase in annual temperature of up to 5°C and an increase of up to 9°C in summer months in 2070–2100 under the A2 scenario, with 1960–1990 as the reference [*Räisänen et al.*, 2004]. Simultaneously, precipitation is expected to decrease slightly throughout the year (−20%), with an enhanced decrease in summer [−50%, *Räisänen et al.*, 2004]. Although climate change impact assessment studies are common, these studies are rare in mountain areas. Several impact studies have been conducted to assess the effects of climate change on mountain hydrology with specific regard to runoff [*Horton et al.*, 2006; *Shinohara et al.*, 2009; *Milner et al.*, 2009], glacier shrinkage [*Paul et al.*, 2007; *Huss et al.*, 2008), snow cover change [*Bavay et al.*, 2009], and more rarely, evapotranspiration [*Calanca et al.*, 2006]. To our knowledge, very few studies have addressed the special explicit impact of climate change on soil moisture in mountain areas: *Jasper et al.* [2004, 2006] studied the impact of different climate models on the hydrologic cycle with a focus on soil moisture, and *Yang et al.* [2009] conducted a sensitivity analysis to evaluate the possible effect of climate change on soil moisture at a coarse scale. This lack of studies contrasts with the key role of soil moisture in ecosystems [*Rodriguez-Iturbe*, 2000]: soil moisture determines the productivity of and nutrient supplies to plants as well as it influences CO_2 uptake, the microclimate, and soil organism reproduction. The reason for this lack of research may be the challenge of simulating soil moisture in a spatially and temporally distinct way. Due to its nonlinear response and the small-scale variability of vegetation, soils [*Gurtz et al.*, 1999], and especially skeleton fractions [*Rössler and Löffler*, 2010; *Poesen and Lavee*, 1994], modeling soil moisture is challenging and is associated with great uncertainties in complex terrains, such as those found in high mountain catchments.

[1]Oeschger Centre for Climate Change Research, Institute of Geography, Group of Hydrology, 3012 Bern, Switzerland.
[2]Department of Geography, University of Bonn, 53115 Bonn, Germany.

0043-1397/12/2011WR011188

[3] *Jasper et al.* [2004] published the most comprehensive study thus far that focused on soil moisture in response to climate change in the Swiss Alps. They found soil moisture storage to be dramatically depleted. Later, *Jasper et al.* [2006] analyzed the spatial pattern of soil moisture decreases at a regional scale and found land use, slope, and altitude to determine the spatial pattern. Climate change impact assessment studies that consider soil moisture in a spatially explicit way are confined to large lowland areas [*Naden and Watts*, 2001; *Holsten et al.*, 2009].

[4] Climate change impact assessment studies at a high spatial and temporal resolution are urgently needed to develop mitigation and adaption strategies at the community level [*Viviroli et al.*, 2011]. This need holds especially true for high mountain catchments where there is high environmental variability over short distances [*Middelkoop et al.*, 2001; *Gurtz et al.*, 1999]. Downscaled global climate models (GCMs) are unable to adequately reproduce this small-scale variability. Hence, several studies [*Jasper et al.*, 2004; *Lenderink et al.*, 2007; *Segui et al.*, 2010] have begun to combine different regional climate models (RCMs) with downscaling approaches to meet the apparent scale mismatch between driving climate models and catchments.

[5] Large uncertainties in climate change impact assessment studies arise from the choice of climate model, emission scenario, and downscaling approach employed [*Wood et al.*, 2004; *Jasper et al.*, 2004). *Bates and Granger* [1969] introduced ensemble forecasting to meet these challenges. This approach produces lower mean errors than single models under the assumption that each model is unbiased. *Ajauro and New* [2007] published a comprehensive review on the different ensemble forecast methods that are available and the overall combination approaches. Forecast ensembles have been used in climate change studies in the areas of climatology [*Stott and Forest*, 2007], land use change [*Viney et al.*, 2009], and hydrology [e.g., *Christensen and Lettenmaier*, 2007; *Bastola et al.* 2011]. Many hydrological studies have simulated ensembles based on different climate models or emission scenarios [*Horton et al.*, 2006; *Jasper et al.*, 2004]. More recently, especially in hydrological studies, the use of a combination of different hydrological models and different climate model data has resulted in highly comprehensive studies [*Christensen and Lettenmaier*, 2007]. Less focus has been directed toward use of a combination of different downscaling approaches with different climate models to drive a hydrological model.

[6] The major challenge of all downscaling approaches is to bridge the gap between the spatial resolution of GCM or RCM outputs and the input data required by the hydrological models. For hydrological modeling, point data from meteorological stations are generally required [*Xu*, 1999; *Fowler et al.*, 2007]. This bridging is basically performed by one of three different approaches: dynamical downscaling, statistical downscaling (SD), or the delta approach, which is also referred to as delta change (Δ). In addition, the direct use (DU) of RCM data has been successfully applied in studies [e.g., *Kunstmann et al.*, 2004]. In the last two decades, several review papers have been published about this topic [cp. *Hewitson and Crane*, 1996; *Wilby and Wigley*, 1997; *Xu*, 1999; *Fowler et al.*, 2007; *Maraun et al.*, 2010].

[7] Unlike mountain areas of arid or semiarid regions, alpine areas in humid temperate zones are not expected to suffer from drought stress [*Körner*, 2003; *Löffler*, 2005; *Viviroli et al.*, 2011]. At a smaller scale, the leeward side effect instead leads to continental dry areas in humid temperate mountains; one example of this is the inner-alpine region of the Alps [cp. *Frei and Schär*, 1998]. Today, sporadic drought is common, resulting in drought stress among coniferous trees in the inner-alpine region [*Rebetez and Dobbertin*, 2004]. Drought stress may have negative effects on forest management and avalanche protection forests [*Schneebeli and Bebi*, 2004; *Teich and Bebi*, 2009]. Further expansion of drought stress may have far-reaching and costly consequences, demanding sound climate change impact assessment studies, especially in the transition zone between dry and moist areas.

[8] To conclude, climate change impact assessment studies addressing soil moisture changes in high mountain areas at the regional scale are highly needed. An ensemble forecast based on different downscaling approaches and climate models is used to meet the uncertainties of each method. Therefore, in this study, we aimed to simulate the impact of climate change on the hydrology and, especially, soil moisture in a mesoscale alpine catchment using an ensemble forecast composed of two RCMs and three downscaling methods. We determined the changes in hydrology and of soil moisture in specific between a reference (1960–1990) and scenario period (2070–2100). We chose a catchment situated at the transition zone between inner dry areas and the very humid central alpine range to evaluate the climate change-induced drought stress potential in areas that are currently dry as well as in areas currently unaffected by drought.

2. Study Area

[9] Detailed spatiotemporal data are needed to simulate soil moisture variability especially in complex mountain areas [*Gurtz et al.*, 1999]. Hence the study area needs to be selected with regard to detailed spatial data available. The present study was performed in a high mountain catchment (*Lötschen valley*, 160 km^2) in the central Bernese Alps in Valais, Switzerland (Figure 1). The Lötschen valley was an investigation catchment within a major research program (GRK 437—Landform) containing several studies with different research foci, e.g., geomorphology [*Welpmann*, 1997; *Eilers*, 2000], vegetation patterns [*Hörsch*, 2001], soil temperatures [*Welpmann*, 2003], and snow depleting dynamics [*Schmidt et al.*, 2009]. Due to the availability of these data and additional meteorological station data from a former project [*Börst*, 2005], a detailed simulation of soil moisture patterns in the *Lötschen valley* seems suitable. But there are some constrains in chosen the study area, like the suboptimal position of the discharge gauge being situated at the center of the valley (Figure 2, right) and accordingly the high dependency of runoff on glacier melt water that influence the model parameterization. Moreover, the uncertainties that come along with changing glacier extent under future climate conditions need to be addressed in such environment. Nevertheless, glaciers are no singularity but typical for most high mountain catchments.

[10] The investigated valley is a northern tributary valley situated in the transition zone between the dry continental inner-alpine valleys of Switzerland and the moist, oceanic northern slope of the Alps. The extent of climate induced

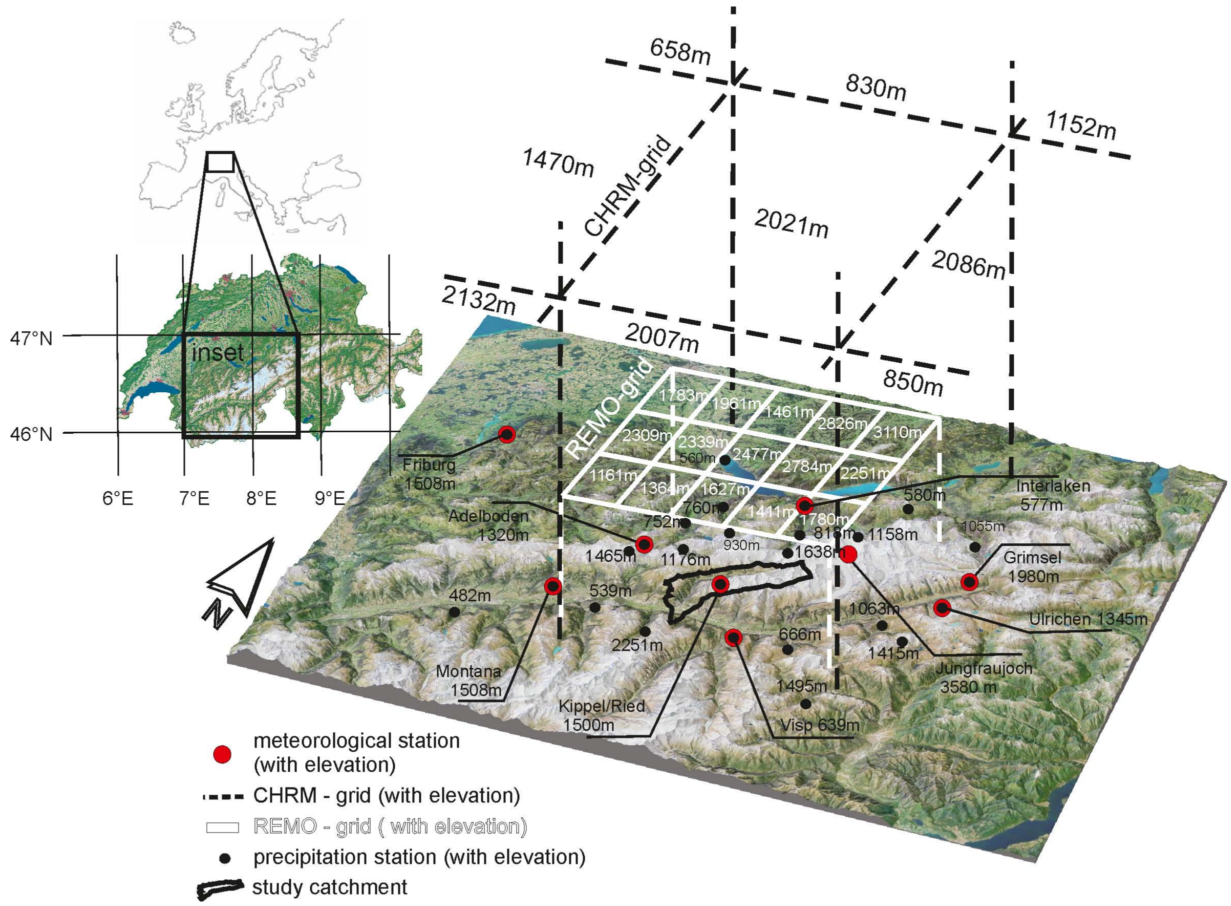

Figure 1. Location of the study catchment in Switzerland, the meteorological stations involved, and the grid cells of the two regional climate models, CHRM and REMO. Background map: Swisstopo.

drought stress potential under climate change conditions is therefore easily assessable. The climate at the center of the valley (1480 m a.s.l.) is characterized by a 4.9°C mean annual temperature and 1120 mm of precipitation, of which 50% falls as snow (all data correspond to 1974–1998 [*Börst*, 2005]). The valley can be subdivided into a wider, largely cultivated valley, in which all of the settlements are situated (hereafter referred to as the main valley), and a steeper, gorge-like area in the south (hereafter referred to as the southern gorge). The elevation of the valley floor ranges from 600 m at the outflow to 2000 m at the glacier tongue. The highest peaks reach nearly 4000 m. Montane deciduous forests are the lowest vegetation unit (1.4%), and they are followed by subalpine coniferous forests (15.7%) intersected by meadows, alpine heath, and grasslands (in total 24.9%) and, finally, nival debris (13.3%), and rocky areas (23.9%) that are sparsely vegetated, as well as glaciers (17.7%) (Figure 2, right). The two major glaciers to the north and to the east are in contact with the glaciers of the adjacent catchments. Rocks and glaciers being characteristic for high mountains area are not informative in terms of climate change impact of soil moisture. An overrepresentation of these land use types should hence be avoided when choosing the study area. Comparing this land use type and the catchment area with other alpine catchments, we found the Loetschen valley to represent almost the mean for Swiss catchments of this altitude (>2300 m mean elevation) in terms of rock and debris (Ø 39.6%), glaciers (Ø 21.1%), and area size (Ø 203 m^2) [cp. *GEOSTAT*, 2002].

[11] The soil distribution was surveyed and their hydraulic properties were derived in a previous study [*Rössler and Löffler*, 2010]. Soils are mainly characterized by a loamy to silty texture and a high, but quite variable, skeleton fraction (Figure 2, left). The soil characteristics vary depending on the parent material; alluvial fans show a higher proportion of sandy material and skeletons, whereas the soil texture of irrigated meadows contains a high fraction of silt due to the century-long history of irrigating these areas with glacier water containing high fractions of silty material (glacier milk).

3. Materials and Methods

3.1. WaSiM-ETH Hydrologic Model

[12] The water balance simulation model developed at the ETH Zurich (WaSiM-ETH) is a frequently used, physically based, distributed hydrological model that was originally developed to simulate climate change effects in Swiss lowland catchments [*Schulla*, 1997]. Later, it was successfully applied to several high mountain catchments [*Gurtz et al.*, 2003; *Verbunt et al.*, 2003; *Jasper et al.*, 2006]. WaSiM-ETH uses spatial data on topography, land cover, and soil properties combined with interpolations of meteorological point data to calculate the hydrological flux and

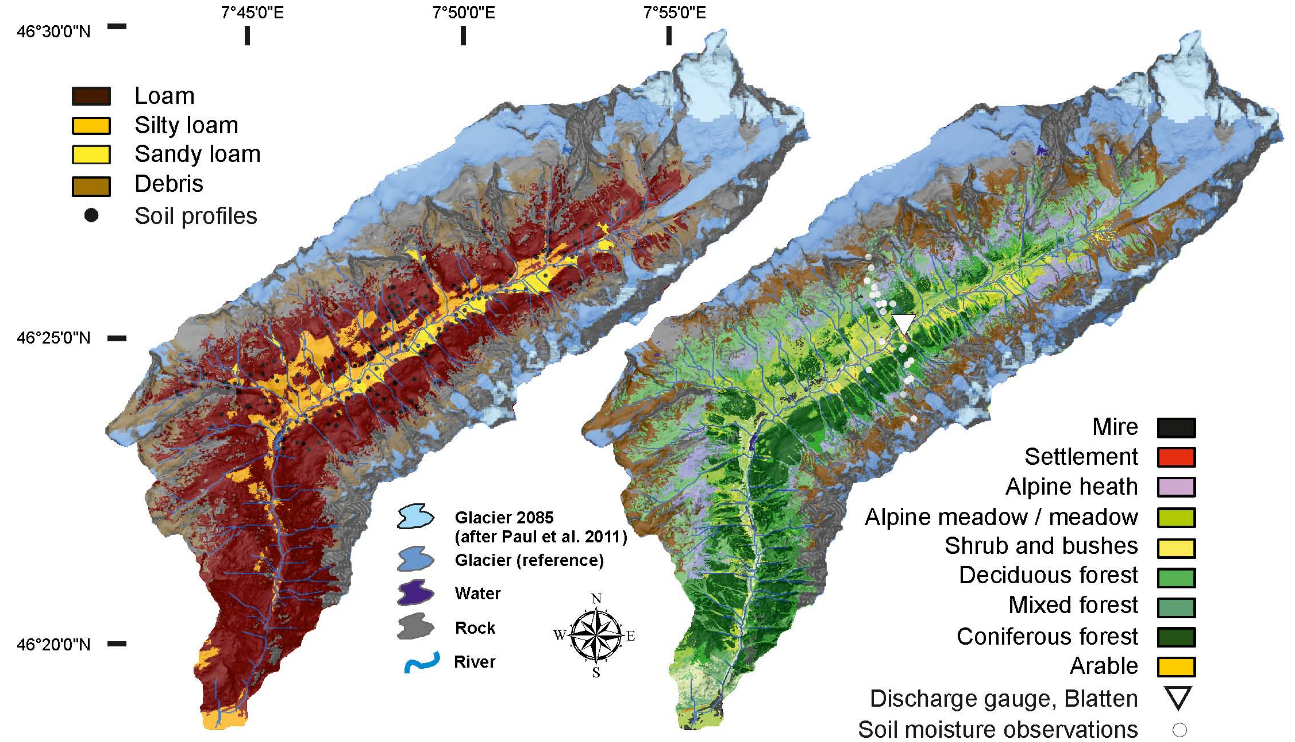

Figure 2. Land cover, rivers, and central runoff gauge (right) as well as the soil texture and parent material distribution (left) within the investigated mountain catchment, the Lötschen valley in the central Swiss Alps.

storage at each raster cell. Lateral fluxes between raster cells are subsequently routed and are expressed in terms of the surface and groundwater flows assigned to the subjacent raster cell with regard to topography based flow times. WaSiM-ETH is not able to rout an interflow from cell to cell, and hence, interflow is directly assigned to the local natural drainage channel under the consideration of the flow time. Infiltration of water into the unsaturated zone is calculated using the approach of *Green and Amp* [1911]. Simulation of the vertical soil water flow is predicted using the Richards equation. In WaSiM-ETH, each soil profile is split into several numerical layers that may consist of different soil properties (soil layers). At the border of these different soil layers, interflow may be generated. In this study, the soil profiles of the first 60 cm are split into six numerical layers of 10 cm each followed by four layers of 30 cm each (60 cm to 180 cm). For groundwater modeling we used a conceptual single-linear-storage approach because empirical data do not exist. The conceptual groundwater model assumes permanent soil water exchange between saturated soils and the groundwater table. Hence, the parameterization of a soil depth ensuring permanent contact with the groundwater table (180 cm) is necessary, but very likely to overestimate the real soil depth in the study area. Base flow generation is done in a conceptual approach since no lateral flows are simulated. For each raster cell base flow is derived from the level of the groundwater table using the following equation:

$$Q_B = Q_0 \, K_S \, e^{\frac{(h_{GW} - h_{alt})}{k_B}}, \tag{1}$$

where Q_B is the base flow (m s^{-1}), Q_0 is the scaling factor for base flow (or maximum base flow if the soil is saturated) (–), K_S is the saturated hydraulic conductivity (m s^{-1}), h_{GW} is the height of groundwater table (m a.s.l.), h_{alt} is the altitude of raster cell (m a.s.l.), and k_B is the recession constant for base flow (m). The parameters Q_0 and k_B have to be calibrated.

[13] Snow and ice storage and melting are important processes within a high mountain catchment. Both processes are modeled in WaSiM-ETH using the degree-day factor algorithm based on *Martinec* [1975]. The snow melting rate is calculated using the following equation (J. Schulla and K. Jasper, Model description WaSiM-ETH (Water balance Simulation Model ETH), 2007, available at http://www.wasim.ch/downloads/doku/wasim/wasim_2007_en.pdf, accessed 30 March 2012, hereinafter referred to as Schulla and Jasper, Model description WaSiM-ETH, 2007):

$$M = c_0 \, (T - T_0) \, \frac{\Delta T}{24}, \tag{2}$$

where M is the melt (mm/time step), c_0 is the degree-day factor [mm/(°C time step)], T is the air temperature (°C), T_0 is the threshold temperature for melt (°C), and ΔT is the time step (h).

[14] The same concept is applied to the snow and ice melt on glacier, but corrected for radiation intensity (equation (3)) following an approach described by *Hock* [1999] as found by J. Schulla and K. Jasper (Model description WaSiM-ETH, 2007):

$$Q_{\mathrm{glac}} = \begin{cases} \left(\frac{1}{n} \, MF + a_{\mathrm{snow}}/\mathrm{ice} \; I_0 \, \frac{Gs}{Is} \right) (T - T_0) \, , & T > T_0 \\ 0 \, , & T \leq T_0 \end{cases}, \tag{3}$$

Table 1. Effective Parameters of the Snow, Glacier and Unsaturated Soil Submodels Used in WaSiM-ETH (cp. Equations (1) and (2))

Submodel	Effective Parameter	Unit	Abbrev.	Value
Snow and glacier modul	Snow melt factor	$mm\,d^{-1}\,C^{-1}$	(C_0)	2
	Glacier melt factor	$mm\,d^{-1}\,C^{-1}$	(MF)	3.9
	Threshold temperature for melt	°C	($T0$)	0.1
	Minimal factor of radiation correction for snow and glacier melt	$m^2\,W^{-1}\,mm\,h^{-1}\,C^{-1}$	(α_{min})	5×10^{-3}
	Maximal factor of radiation correction for snow and glacier melt	$m^2\,W^{-1}\,mm\,h^{-1}\,C^{-1}$	(α_{max})	4×10^{-2}
Soil model	Base flow recession parameter	–	(ks)	0.1
	Scaling factor for base flow	–	(Q_0)	35
	Fraction of snow melt that is direct flow	1/1		0.3
	Drainage density	–		0.1

where Q_{glac} is the glacier melt (mm/time step), MF is the melt factor (–), n is the number of time steps per day (–), α is the empirical coefficient for snow and ice, I_0 is the potential direct incoming shortwave radiation for each grid cell ($W\,h\,m^{-2}$), G_S is the observed radiation at the same time ($W\,h\,m^{-2}$), T is the air temperature in 2 m height (°C), and T_0 is the threshold temperature for melt (°C).

[15] Hence, glacier melt is a direct function of temperature and glacier extent. Glaciers are separately modeled within a specific glacier subcatchment that is additionally routed to the discharge of the downstream subcatchment with no influence on the soil moisture of adjacent subcatchments. In the applied version of WaSiM-ETH (8.0.10), shrinkage of the glaciated is not considered. Therefore, external data of glacier extent is needed to realistically portrayal glacier melt under climate change conditions.

[16] Actual evapotranspiration is modeled in a two-step approach: first, potential evapotranspiration is simulated using the Penman-Monteith equation [*Monteith*, 1975]; second, actual evapotranspiration is derived from potential evapotranspiration by applying the Feddes approach [*Feddes et al.*, 1976], which is a linear reduction that depends on the matrix potential within the root zone. For more detailed information and the equations, see *Jasper et al.* [2006]. Soil hydrological properties are derived based on empirical soil texture data [*Rössler and Löffler*, 2010] and parameterized according to the van Genuchten approach [*van Genuchten*, 1980].

[17] WaSiM-ETH requires spatial data sets of soil hydraulic property units and land use; these soil hydraulic properties were derived from soil properties like soil textures and bulk density using the pedotransfer function (PTF) following *Rawls and Brakensiek* [1985], including consideration of the skeleton fraction (values are given by *Rössler and Löffler* [2010]). The spatial distribution of soil textures (Figure 2, left) was mapped based on 231 profiles and a conceptional approach: a geological map, a geomorphologic map, and an official survey [*GEOSTAT*, 2000] were used to delineate pedogenetically similar soil units that were subsequently specified with soil profiles. The soil textures of each profile were estimated in the field following the method of *AG Boden* [1994] and were verified in the lab for 125 soil samples using Köhn analysis [*Köhn*, 1928]. Land cover was derived from a detailed vegetation map (5×5 m^2) of the Lötschen valley developed by *Hörsch* [2001] and an official land cover survey [*GEOSTAT*, 2002]. Land cover parameters were obtained from Schulla and Jasper (Model description WaSiM-ETH, 2007) and from direct observations in the field (e.g., root depth, vegetation coverage). The main parameter settings are summarized in Table 1. Finally, spatial information on topography was obtained from an official topographic survey [*SWISSTOPO*, 2004]. This information, together with river network data, was used to calculate a hydrologically correct relief [cp. *Davies et al.*, 2007] applying the TOPOGRID algorithm (ESRI).

[18] WaSiM-ETH was successfully calibrated and validated in a previous study [*Rössler and Löffler*, 2010] at an hourly temporal resolution and a 50×50 m^2 spatial resolution. In the cause of this study we adjusted the model to a daily temporal resolution to meet the restrictions of the climate model data used and to keep the computational efforts reasonable. The main parameters of the model at a daily temporal resolution are summarized in Table 2.

3.2. Regionalization

[19] In addition to the data described above, WaSiM-ETH requires spatially distributed information concerning temperature, precipitation, relative humidity, global radiation, and wind speed. Therefore, meteorological station data are interpolated for the catchment for each time step (in our case daily) using linear regression against elevation.

Table 2. Main Land Cover Types of the Study Area and Parameters Used in the Hydrological Model WaSiM-ETH

Land Cover	Leaf Area Index (–) Winter	Leaf Area Index (–) Summer	Albedo (1/1)	Root Depth (m)	Aerodynamic Resistance ($s\,m^{-1}$)	Roughness Length (m)
Coniferous forest	8	12	0.12	0.8	80–55	10
Deciduous forest	0.5	5	0.2	1	90–60	10
Mixed forest	0.3	5	0.15	1	90–60	10
Shrubs and bushes	3	5	0.2	0.3	90–45	1.5–2.5
Alpine meadows/pastures	2	4	0.25	0.4	90–40	0.15–0.4
Alpine heath	2	4	0.25	0.4	90–40	0.15–0.4
Mires	2	4	0.25	0.2	90–40	0.15
Arable land	0	5	0.5–0.25	0-0.4	90–40	0–1

The advantage of this regionalization approach lies in its consideration of the strong altitudinal dependencies of meteorological parameters, which are variable in time. To avoid unrealistic values, a bias correction was applied for each parameter, limiting temperature to between -40 and $40°C$, precipitation to 150 mm d^{-1}, wind speed to 40 m s^{-1} d, radiation to 1000 W m^{-2} d, and relative humidity to 100%. The threshold for precipitation was derived from recent observations in the valley. After a heavy storm in 2005 that caused a major flood in the adjacent Bernese Oberland (Switzerland), a maximal value of 120 mm d^{-1} was observed, and a threshold of 150 mm d^{-1} was derived accordingly.

3.3. Validation of the Hydrological Model

[20] The model was calibrated against discharge in 1960–1975 and validated with the 1975–1990 time period (Figure 3, left). We found the model to show a very good performance as also indicated by the statistical measures ($R = 0.99$, IoA (index of agreement, *Willmott*, [1981]) $=$ 0.99, *ME* [*Nash and Sutcliffe*, 1970] $= 0.97$). As we focus on soil moisture changes, we additionally validated the ability of the hydrological model to reproduce soil moisture within the root zones at a daily resolution (Figure 2, right). Soil moisture data was measured at 15 plots stretching from the valley bottom at about 1450 up to about 2600 m a.s.l. at both sides of the valley in 2006 and 2007 [cp. *Rössler and Löffler*, 2010]. Therefore we simulated the hydrology of the catchment with the calibrated model for these two years and validated the model against observed soil moisture. Figure 3 (center) presents the performance of WaSiM-ETH to reproduce soil moisture and shows a fairly good ($R = 0.63$) agreement with a total error of about 7% vol [expressed as root-mean-square error (RMSE)]. As indicated by the residuals of the linear relationship (Figure 3, right) the model tends to overestimate soil moisture especially at elevation between 1600 and 2100 m a.s.l. while the model mostly underestimate soil water content at higher altitudes. Both findings, the general error of about 7% vol and the error distribution, need to be considered when interpreting the following results.

3.4. Climate Data

[21] Meteorological data from the reference (1960–1990) and the scenario period (2070–2100) were downscaled using the RCMs CHRM, and REMO and applying the A2 scenario and three different downscaling approaches. CHRM is a variation of the Europa Model (EM) from the Institute for Atmospheric and Climate Science of ETH Zurich that is used in climate studies [*Lüthi et al.*, 1996; *Vidale et al.*, 2003]. It provides a grid resolution of 0.5° ($\approx$55 km) and daily time steps. The second regional climate model, REMO [*Jacob*, 2001], Version 5.8, is also based on the EM, but it provides a spatial resolution of $\sim$10 km (0.088°) and individually adjustable time steps, the smallest of which is 1 h. For comparative reasons, we used daily time steps for both models. A major dissimilarity of the RCMs concerns the driving of the GCM, whereas REMO is driven by ECHAM5 and CHRM is driven by HadCM3.

[22] In addition to these climate model data, we used data from several official meteorological stations located within and around the studied catchment that cover an altitudinal gradient from 450 to 3560 m a.s.l. These data were used to calibrate the statistical downscaling (SD) model SDSM 4.2 (C. W. Dawson and R. L. Wilby, SDSM 4.2—A decision support tool for the assessment of regional climate change impacts, 2004, available at http://co-public.lboro.ac.uk/cocwd/SDSM/SDSMManual.pdf, accessed 30 March 2012) and were directly used to drive the reference run of the Δ (delta change) approach. Figure 1 presents the location of the Loetschen valley in Switzerland, the meteorological stations involved, and the extent of the grid cells of both RCMs.

3.5. Spatial Scenario Data

[23] It is widely expected that climate change will very likely cause changes in the occurrence and the distribution of vegetation patterns and shrinkage of glaciers. WaSiM-ETH in its applied version is not able to cope with these

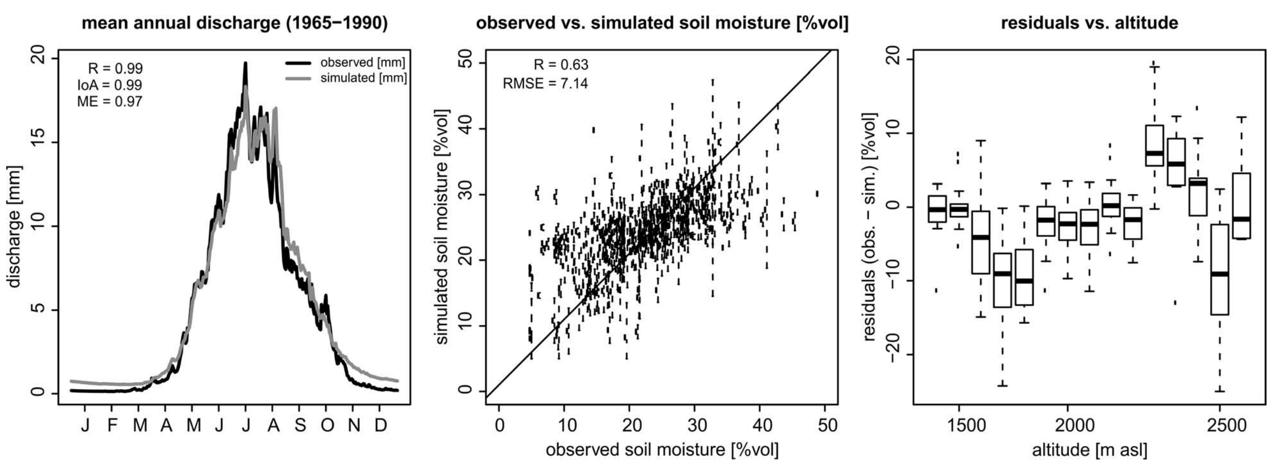

Figure 3. Validation of the hydrological model in terms of mean annual discharge (left) and soil moisture (center). Mean annual discharge was aggregated for the time period 1965–1990 at a daily basis. Soil moisture simulations were lineally compared with observed soil moisture measures from 13 plots from different altitudes (1450 to 2600 m a.s.l.) in 2006 and 2007. Residuals of the soil moisture comparison (right) reveal an overestimation at lower altitudes and an underestimation of higher altitudes.

changes and therefore external data are needed to consider those changes in vegetation and glacier extent. In terms of glacier extent, we made use of the most recent scenario data set available for the Swiss Alps [*Paul et al.*, 2011] with a spatial resolution of 100 m. The glacier extent was simulated based on a glacier-equilibrium-line (GEL) reaction model [*Paul et al.*, 2007] that calculates the glacier extent as a function of temperature induced changes of the equilibrium line. The model uses the downscaled ENSEMBLES data set CH2011 [*Fischer et al.*, 2012] and calculates three different projections based on the overall temperature trend of ensembles member. Due to the scale mismatch between the swiss-wide glacier change study of *Paul et al.* [2011] and the present detailed study of one catchment, we only applied one medium projection of glacier extent: the glacier extent of 2085 as simulated for the medium temperature trend of ensembles members was incorporated in the model for the projection period. That is, since the REMO model being also part of the ENSEMBLE data set is allocated of these medium temperature members. In doing so we were able to portray the future glacier melt and to simulate realistic discharge dynamics. Figure 2 (right) presents the glacier extent under climate change scenario conditions.

[24] In terms of vegetation cover changes caused by climate changes, climate change impact assessment studies are much more challenging, because responses of vegetation patterns might likely be a very slow process [*Dullinger et al.*, 2004]. In addition, *Gellrich et al.* [2007] highlights the impact of socioeconomic drivers during the last decades indicating the relevance of other affecting processes than climate change. Since future land use distribution remains quite uncertain, sensitivity analyses based on different climate and socioeconomic scenarios would be a reasonable approach to analyze the impact of land use change. Such a sensitivity analysis would go beyond the focus of this study and is disregarded this time. Land cover and soil properties distribution are therefore kept unchanged. Only the glacier extend was adjusted according to the study of *Paul et al.* [2011], enabling a realistic portrayal of glacier melt. Areas formerly covered by glaciers are assumed to remain largely uncovered and are treated as debris cover areas with sparse vegetation. Thereby, the new glacier free areas are not considered in the postprocessing, because no information on soil moisture beneath the glacier for the reference period is available.

3.6. Downscaling Techniques

[25] Downscaling of RCM data remains a crucial step in hydrological impact assessment studies [*Fowler et al.*, 2007], and it has been shown that downscaling approaches differ regarding their ability to represent the hydrological processes associated with an investigated catchment [*Wood et al.*, 2004; *Lenderink et al.*, 2007]. The simplest and most popular downscaling approach is the Δ approach [*Arnell and Reynard*, 1996; *Prudhomme et al.*, 2002], which modifies measured data with respect to the related scenario signal. In this study we applied the method of *Köplin et al.* [2010], which smoothed the meteorological observations using the average of a 30 day moving window. This signal is defined as the difference between future and reference climate data. In terms of temperature, Δ signals were added, whereas precipitation values were multiplied by their percentage of change. All other meteorological data (wind speed, relative humidity, and global radiation) remained unchanged.

[26] Statistical downscaling (SD) was performed for all five meteorological variables by applying the statistical downscaling model (SDSM) developed by C. W. Dawson and R. L. Wilby (SDSM 4.2—A decision support tool for the assessment of regional climate change impacts, 2004, available at http://co-public.lboro.ac.uk/cocwd/SDSM/SDSMManual.pdf, accessed 30 March 2012). SDSM can be regarded as a hybrid of a stochastic weather generator and regression-based methods [*Wilby et al.*, 2001] and has been successfully applied in several studies [*Benestad*, 2004; *Khan et al.*, 2006; *Khan and Coulibaly*, 2010]. We used unconditional and conditional (only for precipitation) ordinary least-squares regression and incorporated an autoregression term for all variables. We used a split sampling test to calibrate and validate the statistical model using the period of 1960–1975 for calibration and that of 1975–1990 for validation. The precipitation, temperature, wind, radiation, and relative humidity data of each meteorological station (cp. Figure 1) served as predictands, while the surrounding grid cells for the same variable of each climate model served as predictor variables. We thus took into consideration that the best predictive skill is not necessarily provided by the nearest grid cells, as described by *Brinkmann* [2002]. Each variable was tested for normal distribution before the application of an ordinary least-square regression (OLS) with autoregression. In the case of precipitation, we transferred the predictand and predictor by applying an $x' = \log(x + 1)$ transformation to account for the zero values in the data. Moreover, no autoregression term was introduced for precipitation. Table 3 illustrates the agreement of the absolute sums of the five meteorological variables. We found a good agreement of the observations with CHRM and REMO data for both the calibration and validation periods. Because the predictor-predictant correlation based on monthly regressions was too weak to be applied to future scenario data sets, we calibrated the model against the annual cycle. We thereby achieved linear correlations (R^2) of between 0.36 and 0.54 across all models. In addition, we tested the downscaled precipitation data in terms of dry spell reproduction and found both models to generate a high accuracy of mean (SD-CHRM, $R = 0.83$; SD-REMO, $R = 0.85$) and maximum dry spell lengths (SD-CHRM, $R = 0.61$; SD-REMO, $R = 0.63$) for each meteorological station. Due to a stochastic term in the ordinary-least-square regression [*Wilby et al.*, 2001], SDSM add some variability to the data set and enables the generation of multiple ensemble data sets. In this study we generated 20 ensemble members for each downscaling procedure with SDSM to drive in the hydrological model.

[27] Finally, we used the RCM outputs directly (direct use, DU) as meteorological input data for regionalization and, subsequently, for the hydrological model; each grid cell of the RCM was treated like a meteorological station, and the values were directly interpolated with elevation. Although we found greater uncertainties using this approach than we observed when using the SD approach in a previous study (not yet published), the principal advantage of this approach is that the variability of the climate model data is not modified like for SDSM [*Dibike and Coulibali*, 2006]

Table 3. Validation of SDSM Performance[a]

		Calibration Period			Validation Period		
		Ø–Mean	Ø–Q25	Ø–Q75	Ø–Mean	Ø–Q25	Ø–Q75
Temperature (°C)	obs	4.1	−0.8	9.9	4.3	−1	10
	chrm	3.8	−1.2	8.7	4.4	−0.8	9.5
	remo	4.1	−1	9.1	4.6	−0.26	9.6
Precipitation (mm)	obs	2.7	0	2.6	3.5	0	3
	chrm	3.5	1.7	5	3	1.7	5.1
	remo	3.6	1.7	5.3	3.6	1.7	5.3
Relatively humidity (%)	obs	74.7	64.7	84.4	73.8	63.2	85.9
	chrm	74.8	65.1	84.6	74.4	65.2	84.2
	remo	74.7	64.8	86.5	74.9	64.5	84.8
Global radiation (W s^{-1})	obs	122	58	180	128	64	186
	chrm	125	67	177	129	73	181
	remo	125	70	176	127	72	177
Wind speed (m s^{-1})	obs	3.4	1.5	4.4	3.2	1.7	4.2
	chrm	3.5	1.7	5.3	4.5	2.3	6.5
	remo	3.6	1.7	5.1	3.7	1.7	5.4

[a]Mean and quantiles of absolute values of the five meteorological parameters and the underlying climate model are compared with observations for both calibration and validation period.

and therefore adds considerable value to the analysis. In climate change impact assessment studies in particular, this consideration is crucial because future scenario conditions inherently imply changed climate variability [*Schär et al.*, 2004]. For the same reason, bias correction was not applied, but we checked the plausibility of the elevation-dependent meteorological gradients during 1960–1990, and we found them to be in good agreement with the gradients of the observations (Table 4).

3.7. Analyzing the Effects of Climate Change

[28] Analyses of the impacts of climate change on the hydrology of the valley in general and on soil moisture in particular were carried out in two steps. At first we analyzed the general hydrological impact of climate change based on (1) probability density functions (hereafter PDFs) for selected parameters (Figure 4) and (2) changes in the water balance (Table 5).

[29] Later we compared the changes to the spatial and temporal distribution of soil moisture and actual evapotranspiration, and we compared those differences to changes in temperature, precipitation, and discharge (Figure 5). Special focus was placed on changes in soil moisture (electronic supplement material) and the risk of drought (Figures 6–8). Soil moisture changes were evaluated with respect to seasons, as changes during the vegetated period are much more relevant than those during other seasons.

[30] To measure the occurrence and severity of drought stress, many different drought stress indicators (>100) are present in literature [for review see *Sivakumar et al.*, 2011; *Zargar et al.* 2011]. Most of them referred to meteorological droughts indices at coarse spatio-temporal scales (>1000 km^2 and month). Fewer indices focus on the

Table 4. Mean and SD (Brackets) of Observed and Climate Model Gradients of Precipitation and Temperature Against Elevation

	Observed Mean (SD)	CHRM Mean (SD)	REMO Mean (SD)
Precipitation (mm/100 m)	0.165 (0.37)	0.128 (0.44)	0.149 (0.39)
Temperature (K/100 m)	−0.55 (0.11)	−0.58 (0.14)	−0.61 (0.14)

agricultural drought that is much more relevant for plants at much finer scales. These indices are mostly based on results of hydrological models, because detailed spatial data on soil moisture are needed. We decided to calculated three different indicators to evaluate the occurrence of drought stress within the valley. First, we focus on the annual dynamic of drought stress and made use of the reduction of evapotranspiration resulting from increased suction pressure [after *Feddes et al.*, 1976, see above] by determining the evapotranspiration deficit [actual evapotranspiration (ETA)/potential evapotranspiration (ETP)]. This evapotranspiration deficit has been frequently employed as an indicator of drought stress [*Jasper et al.*, 2004, *Jasper et al.*, 2006] or in slighty different form by *Matera et al.* [2007] and *Narasimhan and Srinivasan* [2005]. Second, *Jasper et al.* [2006], in accordance with *Allen et al.* [2010], defined thresholds of 30% (severe) and 50% (moderate) of field capacity as critical levels. For comparative reasons, we adopted the 30% threshold and counted the consecutive number of days for which the simulated water availability was below this level. Third, we introduced a new index (weighted deficit sum, WDS) that considers the evapotranspiration deficit ratio (ETA/ETP) as well as the absolute deficit (equation (4)): For each time step (daily resolution) we calculated the absolute differences between the potential and actual evapotranspiration, weighted this value by the magnitude of the evapotranspiration deficit, and summed them up:

$$WDS = \sum_{i=1}^{n=11322} \left(\frac{ETA_i}{ETP_i} \right) (ETP_i - ETA_i), \tag{4}$$

where WDS is the weighted deficit sum, ETA is the actual evapotranspiration (mm d^{-1}), ETP is the potential evapotranspiration (mm d^{-1}), and n is the number of simulated time steps (d).

[31] The major advantage is that the index (WDS) considers the magnitude of potential evapotranspiration, in other words drought stress on hot days count more than drought stress during winter.

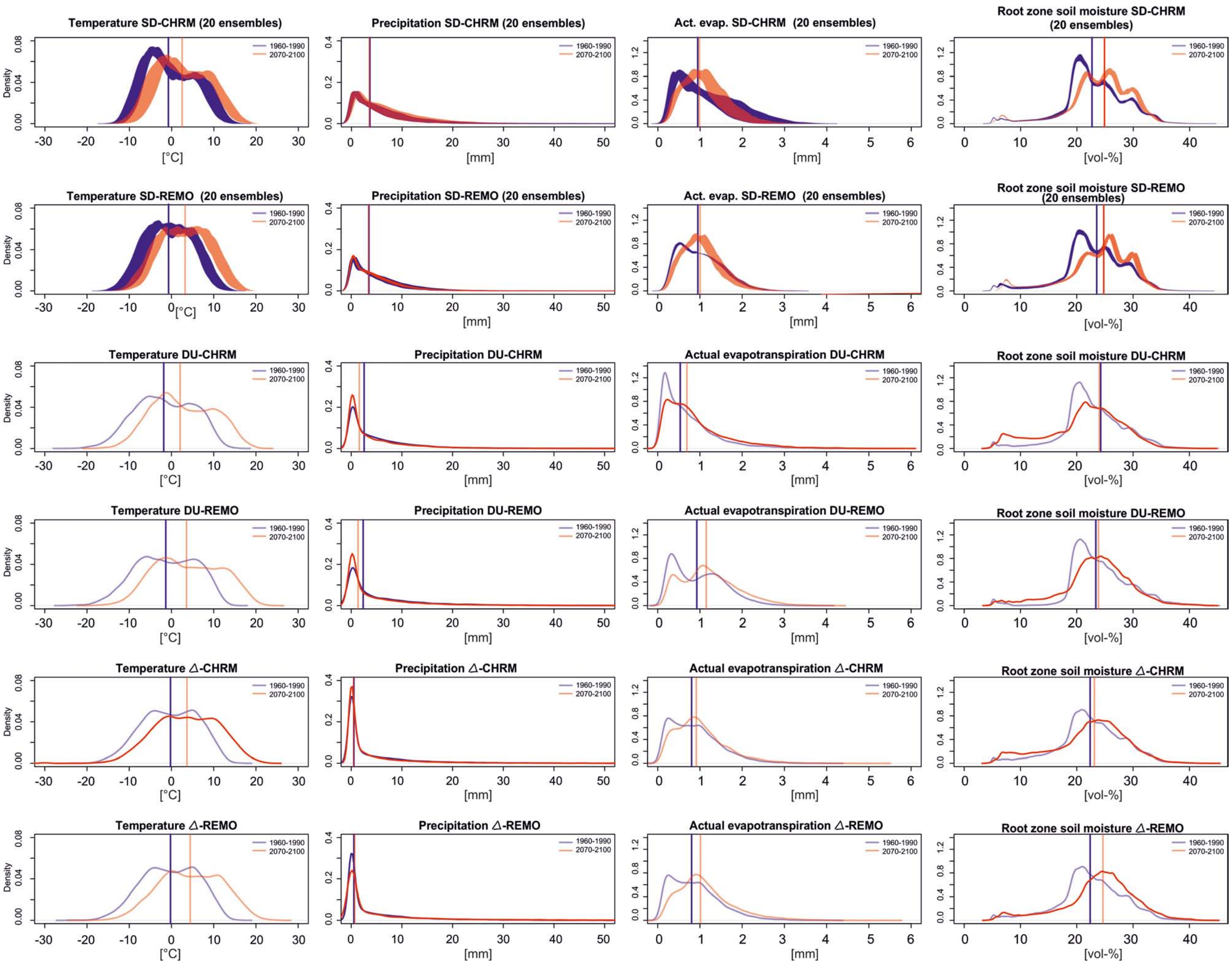

Figure 4. Comparison of reference (1960–1990, blue) versus scenario (2070–2100, red) periods for temperature, precipitation, actual evapotranspiration, and soil moisture for CHRM and REMO as well as three downscaling techniques (SD, DU, and Δ). Shaded areas indicate the 20 ensembles conducted in the SD approach.

3.8. Ensemble Forecasting

[32] Ensemble forecasts are widely used to achieve robust simulations. Depending on the total number of simulations conducted, ensemble forecast analyses range from simply averaging forecasts and evaluating their variability using bounding boxes to much more sophisticated approaches analyzing the probabilities of forecasts [*Araujo and New*, 2007]. For the latter type of approach, a large number of ensembles is necessary, which exceeds the computational capacity of most physically based, distributed models. In this study we simulated 20 ensembles based on the SD approach and performed one model run each of Δ and DU to evaluate the general impact on hydrology (water balance, discharge, evapotranspiration deficit). In terms of the spatial differences involved in climate change impact assessment, computational and storage shortages forced a restriction to only one SD model. Therefore we chose the model with the least deviation from the ensemble mean in terms of precipitation and temperature. The spatial consensus of the six model runs (two regional climate models downscaled using three downscaling approaches) was estimated by arithmetic means and, variability was analyzed using 0.25 and 0.75 quantiles.

4. Results

4.1. Climate Change Impact on the Hydrologic Cycle

[33] The impact of climate change on the hydrologic cycle is most concisely summarized as changes to the probability density function of hydrological variables (Figure 4). Depending on the climate model and downscaling approach employed, slightly different temperatures and precipitation distributions were simulated, which led to varying magnitudes of change in the actual evapotranspiration and monthly soil moisture values.

[34] The temperature distributions for all six ensembles shifted for the scenario period by several degrees under all model approaches applied. High temperature values show a stronger shift than low temperatures. This difference was even more pronounced when applying REMO climate models. In addition, an expected flattening of the curves under scenario conditions, indicating increased variability,

Table 5. Effects of Climate Change on the Water Balance With Respect to the Two Regional Climate Models and Three Downscaling Techniques, Expressed As the Annual Mean and Sum Values, Respectively, As Well As the Percent Change[a]

		Temp. (°C)	Summer Temp. (°C)	Precip (mm)	Total Runoff (mm)	Runoff A Turn Gauge (mm)	Snowfall (mm)	Rain (mm)	Evapotranspiration (mm)	Snow Storage (mm)	Glacier Balance (mm)
1960–1990	SD-CHRM	−0.15 ↑	5.5 ↑	1534 →	1248 →	1476 →	917 ↘	617 ↗	388 →	62 ↓	−1732 →
2070–2100	SD-CHRM	2.5	8.1	1527	1294	1609	671	856	365	6	−1605
	(% Δ)			−0.5	3.7	9.0	−26.8	38.7	−5.9	−90.3	−7.3
1960–1990	SD-REMO	−0.17 ↑	4.56 ↑	1410 →	1073 →	1247 ↗	824 ↘	585 ↗	377 →	69 ↓	−1141 ↘
2070–2100	SD-REMO	2.47	7.0	1383	1149	1441	561	823	359	3.7	−1302
	(% Δ)			−1.9	7.1	15.5	−31.9	40.7	−4.8	−94.6	−14.1
1960–1990	DU-CHRM	−1.38 ↑	5.04 ↑	1482 →	1251 →	1401 →	876 ↘	606 ↗	267 ↗	65 ↓	−2768 ↓
2070–2100	DU-CHRM	2.26	9.2	1371	1231	1529	698	672	308	1	−4662
	(% Δ)			−9.3	−1.6	9.1	−20.3	10.9	15.3	−98.5	−68
1960–1990	DU-REMO	−1.11 ↑	5.43 ↑	1939 →	1567 →	1606 ↗	1202 ↘	739 ↗	368 ↗	53 ↓	−2434 ↓
2070–2100	DU-REMO	3.25	10.6	1761	1498	1711	794	966	423	3.8	−6587
	(% Δ)			−9.1	−4.4	6.5	−33.9	31.3	14.9	−92.8	−171
1960–1990	Reference	−0.3 ↑	5.38 ↑	1418 ↗	1239 ↗	1471 ↗	907 →	510 ↗	326 →	42 ↓	−2345 ↓
2070–2100	Δ-CHRM	2.95	9.35	1785	1710	2143	1030	755	342	−11	−7702
	(% Δ)			25.8	38.0	45.7	13.5	48.0	4.9	−126	−228
1960–1990	Reference	−0.3 ↑	5.38 ↑	1418 ↑	1239 ↑	1471 ↑	907 ↗	510 ↑	326 ↗	42 ↓	−2345 ↓
2070–2100	Δ-REMO	3.74	10.2	2466	2412	2953	1209	1258	384	−3	−8697
	(% Δ)			73.9	94.7	100.7	33.3	146.7	17.8	−107.1	−271

[a]Arrows indicate the magnitude of change.

was barely detectable. Differences in precipitation amounts were restricted to medium values. In contrast, the DU models and Δ-CHRM were characterized by an increase in low precipitation amounts under the future scenario. For Δ-CHRM, this increase can be attributed to an increase in the number of values slightly higher than zero. Changes in the variability of precipitation amounts were negligible. Only Δ-REMO showed a decrease in low precipitation amounts under the future scenario conditions (Figure 4) and higher total amounts of precipitation (cp. Table 5).

[35] The impacts of changed meteorological conditions on noncryospheric water were illustrated by changes in actual evapotranspiration and soil moisture. The PDFs of actual evapotranspiration showed similar changes under the future scenario conditions for all six approaches. We found a shift of low actual evapotranspiration sums ($\ll 1$ mm d^{-1}) to values of approximately 1 mm d^{-1}, while the median remained nearly unchanged. This shift was not achieved by DU-CHRM. In addition, the highest evapotranspiration values remained unchanged, except for in the Δ models, which showed higher extreme values. In terms of soil moisture, all model approaches showed an approximately unimodal distribution characterized by a mean probability density of ±20 vol%. Under future scenario conditions, a distinct flattening of the density curve occurred, indicating increased variability, and was accompanied by a rise of the mean density from 20 to 25 vol%. The main differences between the model approaches were changes in the lower and upper values of the density function: both SD models and the Δ-REMO model showed a distinct increase in density for values of 25 and 30 vol% and no change in the lower soil moisture values. In contrast, both DU models and the Δ-CHRM approach revealed an increase in the densities of values from 20 to 7 vol%, indicating a shift to much drier conditions under the future scenario conditions. Applying the Δ-REMO approach, this soil moisture depletion trend could not be traced. Increases in soil moisture median value as found especially for Δ approaches have to be interpreted as a result of increased snow melt and precipitation in spring and winter, as well as in highest altitudes (cp. Figure S1). In summary, we largely found similar functions and changes regarding the PDFs that resulted in a two-part response in terms of monthly soil moisture: a strong depletion (DU models and the Δ-CHRM approach) or a shift to even moister conditions (SD models and the Δ-REMO approach).

[36] Next, the impact of climate change on the water balance was calculated (Table 5). For the SD and DU models we found a strong increase in temperatures and unchanged precipitation amounts, which caused a shift from snow to rainfall, enhanced ablation of snow and enhanced glacier shrinkages, and only slightly if even increased discharge sums. For the Δ models, increasing temperatures and increasing precipitation amounts led to a strong rise of discharge amounts, especially those of Δ-REMO. The overall pattern of the results for the water balance emphasizes that the particular downscaling technique used is of greater importance than the climate model applied. In addition, major differences were caused by different precipitation amounts, whereas deviations in temperature increases were negligible.

[37] In a further step, changes to meteorological and hydrological parameters were analyzed with regard to the

intra-annual deviations between reference and scenario runs. The plots indicated that temperature increase is more equally distributed throughout the year compared to the precipitation changes for all model approaches (Figures 5a and 5b) that were predominantly apportioned to the winter months (Figure 5b). This result explains the trend toward higher snow fall sums found for the Δ models (Table 5). Meteorological changes led to a shift in discharge dynamics: under reference conditions, all model approaches produced a single-peaked curve representing a glacionival discharge regime, while under future scenario conditions this discharge characteristic was advanced by 1 month and showed slightly smaller maximum discharge values as a result of decreased snow storage. Accordingly, the Δ approaches showing a snow fall increase, revealed a smaller if any temporal shift, and an increase of maximum discharge. In addition, noticeable increase in winter discharge was found for all ensembles.

[38] The differences between the reference and future scenario conditions in terms of monthly mean soil moisture showed a strong dependency on the preceding snow melt processes; the future soil moisture surplus corresponds to earlier snow melt, followed by a loss of soil moisture during snow melt in the reference model. This behavior can be found at different magnitudes for all model approaches. For SD models showing the least change in precipitation and temperature, we consequently found only small changes in soil moisture dynamics. However, these small changes had a major impact on actual evapotranspiration. Evapotranspiration was significantly reduced during summer for some areas under SD-CHRM. The DU models produced the strongest temperature increase and decreasing summer precipitation, resulting in the largest differences both for soil moisture and actual evapotranspiration. Accordingly, soil moisture significantly decreased in summer, and concurrently, the actual evapotranspiration values increased. The large variability in the values expressed by the wide range of hinges indicated that enhanced evapotranspiration was driven by temperature and that the evapotranspiration deficit was caused by dry soils. The Δ models showed intermediate differences, particularly in terms of soil moisture, which increased during winter and decreased to some extent in summer. For the Δ-CHRM approaches, we found a soil-drought-dependent evapotranspiration decrease in parts of the valley, as indicated by the lower hinges.

[39] In conclusion, we observed earlier discharge under climate change conditions, indicating that earlier snow melt caused earlier changes in soil moisture dynamics and an increase in winter discharge. Moreover, we found some evidence that evapotranspiration was reduced due to soil drought during summer in some parts of the study area.

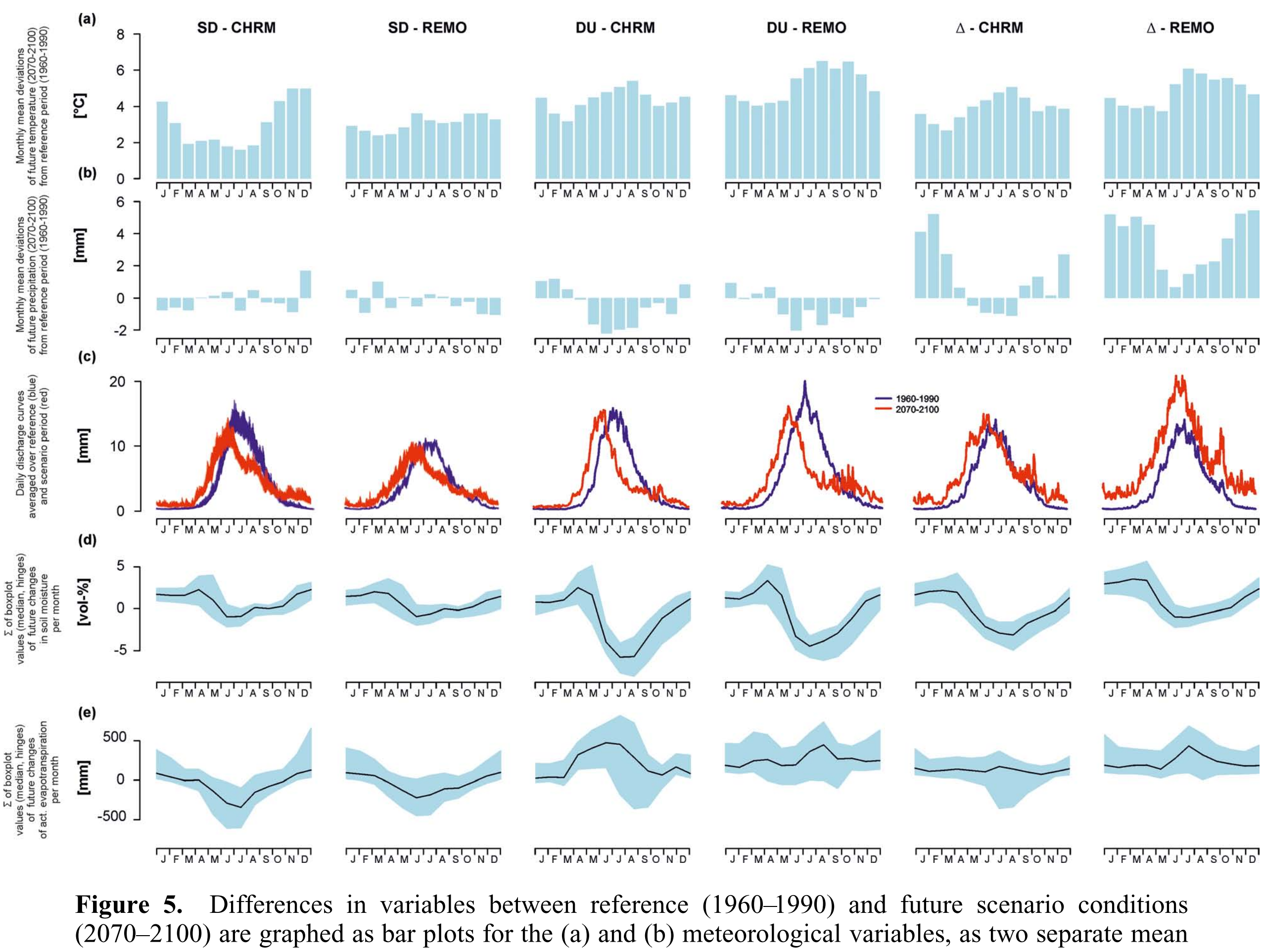

Figure 5. Differences in variables between reference (1960–1990) and future scenario conditions (2070–2100) are graphed as bar plots for the (a) and (b) meteorological variables, as two separate mean annual curves of (c) "terrestrial" discharge (blue and red), and as differences in the spatial distribution of (d) soil moisture and (e) actual evapotranspiration expressed as medians and hinges.

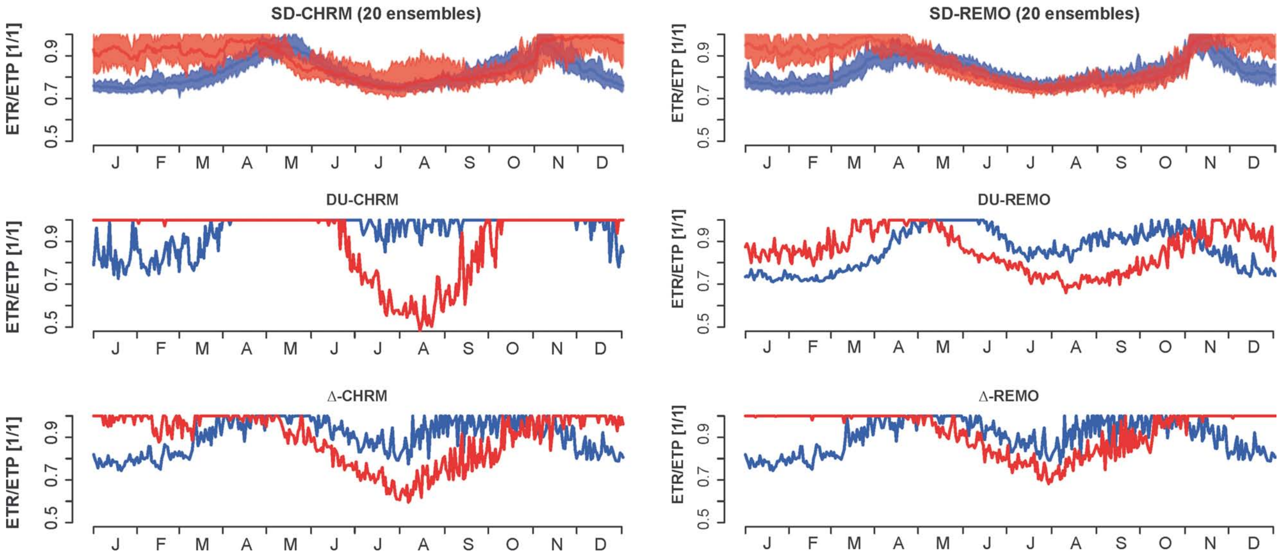

Figure 6. Comparison of the averaged evapotranspiration deficit in the studied catchment based on three downscaling methods and two regional climate models. Blue curves indicate the evapotranspiration deficit under reference conditions (1960–1990), and red curves indicate the deficit under future scenario conditions (2070–2100). Shaded areas indicate the range of ensembles conducted in the SD approach, and thick lines indicate the ensemble mean.

[40] To verify this soil-drought-dependent evapotranspiration decrease and to analyze the impact of climate change on soil droughts in general, we calculated the evapotranspiration deficit for the reference and future scenario conditions (Figure 6) based on daily means for the entire catchment. We found a strong increase of the evapotranspiration deficit during summer for the DU and Δ models under the future scenario conditions; DU-CHRM was characterized by the highest soil moisture depletion (Figure 5d). Furthermore, the magnitude of the enhanced evapotranspiration deficit found for the different models corresponds to the magnitude of the decrease in soil moisture. In contrast, the enhanced evapotranspiration deficit expected in summer for SD-CHRM could not be confirmed.

4.2. Climate Change Impact on Soil Moisture

[41] The impact of climatic change on soil moisture patterns is basically illustrated by the differences in the seasonal means of soil moisture, which were based on daily records. A comprehensive figure in the auxiliary material (Figure S1) presents the results of all six model approaches and the consensus of the models as expressed by the mean and the 0.25 and 0.75 quantiles.[1]

[42] For all seasons we found the differences between the downscaling approaches to be much higher than those between the applied climate models. The largest decrease in the future soil moisture conditions was found for the DU models across all seasons. In summer, in particular (JAS), declines of up to 25 vol% were simulated at the south facing slope and for the grasslands of the valley floor that exhibited high soil moisture content in the reference simulation. This depletion lasted until autumn (OND). In contrast, the SD models provided a rather conservative simulation of the impact of climate change on soil moisture. Excluding the steep gorge, we found no noteworthy depletion of soil moisture ($<-2\%$) and nearly no increase in nonforested areas during winter ($<+5\%$). The Δ models revealed an increase in soil moisture (+5%) in all parts of the catchment during winter (JFM), whereas we found no major change in soil moisture in all other seasons.

[43] Accordingly, the consensus of the model approaches revealed a rather slight change in soil moisture, but great variability with respect to the model applied. We found an increase in soil moisture during winter (JFM), with a maximum being observed for grasslands at the south facing slope. During spring (AJM), large areas were slightly drier under the future scenario conditions, whereas the highest elevations showed an increase in soil moisture. The soil moisture decline was highest in summer (up to 5 vol%), mainly affecting the forested areas on the south facing slope. In addition, the 0.25 and 0.75 quantiles indicated a high degree of variability in the ensemble modeling, ranging from nearly no change in summer and a considerable increase in soil moisture in winter to depletion in summer (5% to 10%) and a slight decrease in soil moisture during winter. This wide range of changes in soil moisture calls into questions the interpretability and the relevance of soil moisture in climate impact assessment studies. Therefore, a more detailed, day-to-day analysis was conducted to evaluate the impact of climatic change on soil moisture and drought stress at a higher temporal resolution.

[44] We analyzed the length of drought stress and its variation under climate change conditions (Figure 7). Thereby drought stress was defined as 30% of field capacity. The DU and Δ models showed a much stronger depletion of soil moisture than the SD models that provided a more conservative response. Although most parts of the valley (DU-CHRM, Figure 7), or at least the forested areas (DU-REMO, Figure 7), experienced short-term drought

[1]Auxiliary materials are available in the HTML. doi:10.1029/2011WR011188.

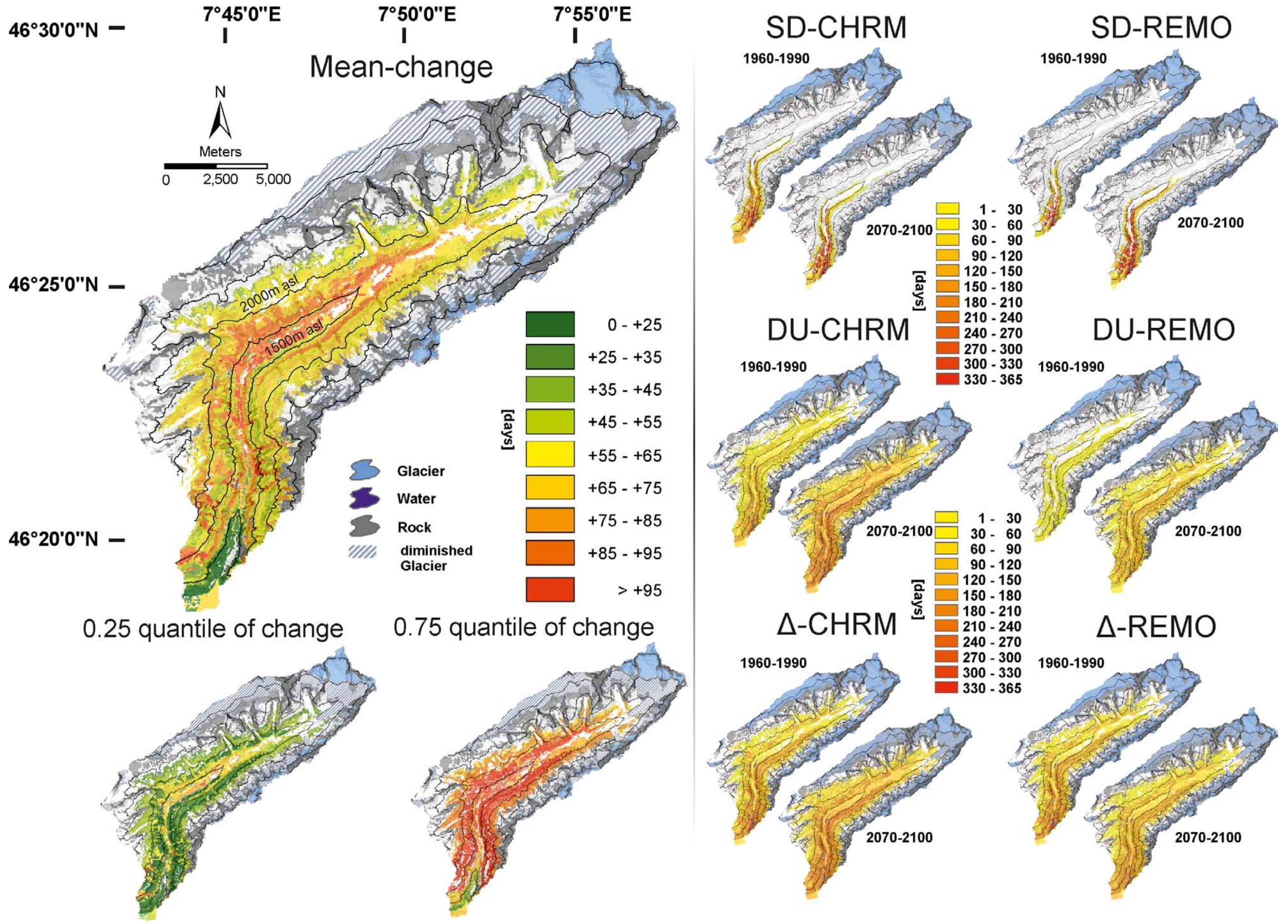

Figure 7. Maximum of successive days in which the soil moisture drops below the critical level of 30% of the plant available water for each model under reference and future scenario conditions (right) as well as the model consensus for the differences between the conditions.

stress during the reference period, a distinct increase in the drought stress duration was simulated with the DU and Δ models. CHRM-driven simulations revealed an enhanced drought stress signal. Although a slight increase in length was also detectable with the SD models, desiccation affected only a limited area at lower altitudes. In general, the consensus of the differences among the six models revealed a considerable lengthening of the drought stress duration, which was amplified for nonforested areas. The increase in nonforested areas is ascribed to the higher potential to lengthen the drought stress duration because of their higher soil moisture value under reference conditions. The strong lengthening trend found in the consensus is accompanied by a high degree of variability in the simulation, as indicated by the quantiles; while a duration at least of 30 days is likely (0.25 quantile), a dramatic lengthening of 90 days or more can also be expected (0.75 quantiles).

[45] In general, the WDS values (Figure 8) confirmed the pattern of the previous analysis, but it further elucidated the impact of climate change on soil moisture and the differences between the model approaches. The strongest increase (150%, + 2300 mm) in the WDS under the future scenario conditions was found for the DU models. This increase was simulated especially for forested areas up to an elevation of 2000 m a.s.l. (Figure 8). The grasslands and all higher elevations (>2000 m a.s.l.) exhibited little change. The WDS values of the Δ models were in line with the pattern found for the DU models, but with lower increases (100%, 1500 mm). Only the SD models revealed much lower WDS values and small changes, excluding some changes in the southern gorge. The consensus of the models followed the pattern of the DU and Δ models by depicting large increases in the evapotranspiration deficits for all of the forested areas in the valley at lower and medium elevations (<1800 m a.s.l.). Due to the deviant simulation of the SD models, the variability of the models was very high, ranging from nearly no change to 2500 mm WDS.

[46] As we found strong evidence that the downscaling approach instead of the underlying climate model is of much higher importance to the model result, we tested the impact of these two factors on the results presented. Following *Finger et al*. [2012], we conducted a two-way ANOVA to analyze the relative importance of both downscaling approach and climate model to the total variability of climate change induced changes in WDS, drought stress length, soil moisture depletion, discharge (Table 6). The influence is presented as the ratio of the summed squares of changes for each hydrological feature. The ANOVA confirmed the visual guess that the variability of changes of

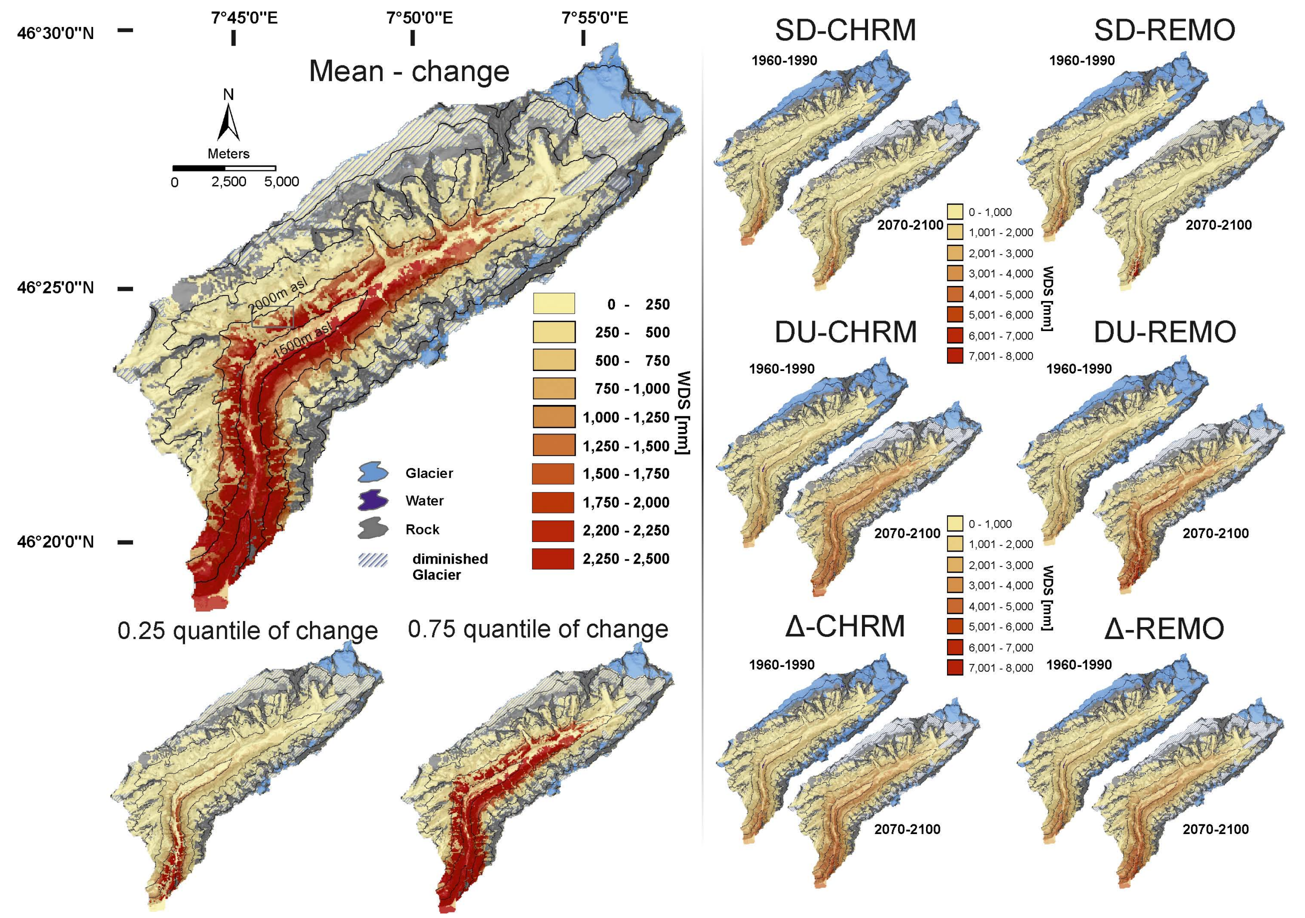

Figure 8. The weighted deficit sum (WDS, cp. equation (1)) for the different model approaches and the model consensus for changes, as expressed by mean and quartile values.

drought stress length and WDS is cause first of all by the downscaling approach applied. In terms of discharge, the influence of the downscaling approach is not as relevant (0.45): The ratio of summed squares of residuals, containing interactions of both factors as well as unexplained variance, is considerably high, indicating the increasing influence of climate models and interactions between both factors. Strikingly, the influence of the downscaling approaches was found to be much smaller in terms of the variance of absolute soil moisture change that is based on monthly values. Due to the contextual similarity, we refer the difference in driving factors between soil moisture and WDS and drought length, respectively, to the temporal resolution of analysis. Soil moisture depletion was analyzed at a monthly basis, while WDS and drought stress length was calculation on a daily basis.

Table 6. Analysis the Influence of Downscaling and Climate Model on the Simulation Variability of WDS, Drought Stress, and Discharge; Expressed As Ratio of the Sums of Squares (Two-Way-ANOVA)

	Ratio of Sum of Squares (–)		
Summed Absolute Values of Change for	Downscaling Approach	Climate Model	Interactions/ Residuals
WDS	0.66	0.15	0.19
Drought length	0.66	0.18	0.16
Discharge	0.46	0.24	0.3
Soil moisture	0.27	0.44	0.28
Summer soil moisture	0.35	0.24	0.41

[47] We assumed that the strong variability in drought stress—that was traced back to the downscaling approach applied—might be ascribed to the representation of the dry spell frequency in the area precipitation as simulated by the hydrological model (Table 7). Apparently the SD models are unable to either reproduce dry spell length of the reference run or presume the dry spells length of the climate model under climate change conditions. DU and Δ approaches in contrast show overall quite similar lengths of dry spells: Slight increases of mean and maximum dry spell lengths under climate change conditions are found for DU and Δ downscaling approaches, with CHRM models having somewhat higher values.

[48] To summarize, statistical downscaling (SD) was associated with a very conservative estimation of future hydrology and soil moisture, whereas the direct use (DU) and delta change of climate models resulted in stronger changes. In addition, we found a drastic decrease in snow and ice storage, earlier discharge, and nearly unchanged evapotranspiration totals. Soil moisture depletion at a seasonal resolution changed little. However, strong effects on the evapotranspiration deficit and drought stress were found on a daily scale; forested areas at elevations below 1800 m were most affected. However, the ensembles revealed such

Table 7. Dry Spell ($p < 1$ mm d^{-1}) Lengths of the Climate Models and the Three Downscaling Methods As Simulated in the Hydrological Model Indicate the Similarity of Climate Model Outputs, But the Inability of the SD Approach to Portray the Dry Spell Length of Observations and Models

	1960–1990					2070–2100					
	Refer.	SD-CHRM	SD-REMO	DU-CHRM	DU-REMO	SD-CHRM	SD-REMO	DU-CHRM	DU-REMO	Δ-CHRM	Δ-REMO
Max	36	9	9	31	29	9	10	37	35	42	38
Q75	4	2	2	4	3	2	2	4	4	4	4
Mean	3.1	1.5	1.5	3	2.7	1.5	1.5	3.4	3.1	3.3	3.15
Median	2	1	1	2	2	1	1	2	2	2	2
Q25	1	1	1	1	1	1	1	1	1	1	1
Min	1	1	1	1	1	1	1	1	1	1	1

high variability that the results should be questioned. This variability was attributed to differences in temperature and precipitation (Figures 5a and 5b) and in terms of drought stress to the representation of dry spells.

5. Discussion

[49] The application of an ensemble forecast involving two RCMs and three downscaling approaches revealed that summer drought stress increased strongly under future climate conditions, particularly at lower elevations and in forested areas. This depletion was accompanied by a wide range of possible scenarios, ranging from stark decreases (+85 days prolonged drought stress, and +150% WDS) to nearly unchanged conditions, depending on the regarded ensemble member. This finding adds considerable value to the discussion regarding the uncertainties and variability involved in climate change impact assessment studies. The use of multiple downscaling techniques in an ensemble forecast represents a novel approach for soil moisture impact studies. Ensemble forecasts are typically conducted with several climate models and emission scenarios and apply only one downscaling technique. These simulations have produced contrasting results: *Zierl and Bugmann* [2005] found large effects on uncertainties for climate models and emission scenarios. *Jasper et al.* [2004] emphasized the superior role of scenarios, whereas *Horton et al.* [2006] and *Wilby and Harris* [2006] found different climate models to cause greater variability in the results. The current study demonstrated a superior role of downscaling approaches in the models' results as well as questioned the validity of forecasts based on a single downscaling approach.

[50] Furthermore, in the current study, statistical downscaling was associated with a highly conservative estimation of future hydrology and soil moisture, with the fewest changes being observed when using this approach. In contrast, direct use (DU) of climate models revealed particularly strong changes. Deviations between DU and Δ on the one hand and SD on the other hand occurred in temperature, indicating the inability of SD to reproduce the changes in variability in climate models under future conditions [*Schär et al.*, 2004]. The loss of variability that occurs during the downscaling procedure is one of the major disadvantages of statistical downscaling [*Wilby et al.*, 2001; *Dibike and Coulibali*, 2006; *Fowler et al.*, 2007; *Maraun*, 2010]. Additionally, in the present study, SDSM calibration was performed based on the annual cycle, disregarding seasonal or monthly changes in the predictor's weight. These two limitations might be one explanation for the conservative simulation of changes.

[51] More importantly, we found SD approach to be unable to reproduce dry spell length of climate models. This finding was all the more interesting as we tested the ability of statistical downscaling to reproduce dry spell length of meteorological stations (section 3.6). The reason for the deficiency in the modeling process had to be ascribed to the single-site character of the weather generator implemented in the downscaling model SDSM. In combination with the applied interpolation for all meteorological stations (daily), the model largely overestimated rain fall events since a dry spell seldom occurred at all stations at once. *Wilby et al.* [2003] published a workaround to use SDSM in a multisite character: An area-average precipitation pattern or patterns of a single site were used as a marker that defines precipitation occurrence in the area and the amount of precipitation was afterward resampled from the area-average distribution. The disadvantage of this approach was that the precipitation can never exceed observed rainfall [*Haylock et al.*, 2006] and it was questionable if the area-average precipitation pattern was suitable for complex mountain terrain like in our study. Nevertheless, further studies need to consider the multisite suitability of the applied weather generator. In contrast to the SD approaches, the DU approaches showed quite similar dry spell lengths than the reference run and a slight increase under climate scenario conditions. The Δ approach being just a scaled reflection of past dry and wet spell patterns revealed similar lengths to the reference and the DU approach, too. The slight increase in future dry spell length was interpreted as an undercut of the defined threshold for a dry spell (1 mm d^{-1}, Table 7). More sophisticated statistical downscaling approaches, such as quantile mapping [*Themessl et al.*, 2011] and artificial neural networks [e.g., *Segui et al.*, 2010], might generate better results in future studies.

[52] On the contrary, the DU models generated the strongest change as a result of decreasing summer precipitation (Figure 5) as well as the longest average dry spells (Table 7). How certain are these results? It is known that DU of RCMs is prone to biases in the climate model [*Kunstmann et al.*, 2004; *Bosshard et al.*, 2011]. However, the main advantage of this approach lies in the application of unchanged model outputs with least loss of variability, resulting in the most reliable differences in dry spell lengths under reference and future scenario conditions. *Frei et al.* [2003] comprehensively analyzed RCM performances and showed that both applied RCMs (CHRM

and REMO) tend to underestimate summer mean precipitation by 25% and related this bias to a too less intensity, a too short frequency distribution, and too short dry spells in comparison to observations. The underestimation of summer precipitation is also found in DU approaches (Figure 5b) and the climate model limitations in terms of intensity and frequency are partly underpinned by the regionalization regression applied, which tends toward mean values. In summary, although DU of RCMs has been reported to be associated with numerous biases originating from the RCMs, it is able to maintain the information of the RCMs with least loss of the important variability.

[53] *Graham et al.* [2007] found the Δ approach to produce coherent results that preserve changes in the variability of climate models. We argue that this preservation can only be partly achieved due to the scaling character of the Δ approach. Especially, changes in dry and wet spell frequencies are not adequately considered in this approach. This statement is in line with the findings of *Lenderink et al.* [2007], who compared the DU and Δ approaches. Moreover, the Δ approach showed strong deviations in terms of precipitation that were caused by using the moving average to derive the Δ signal and the resulting high Δ change factors. While this might be a bias from the method applied, RCM limitations described for the DU approach hold also true for the Δ approach. Therefore the reliability of the Δ change method, at least in terms of soil moisture studies, has to be questioned. To conclude, each of the applied downscaling methods has strong limitations and according to *Frei et al.* [2003] both RCMs reveal model biases in terms of summer precipitation that need to be considered when interpreting the result of the simulation.

[54] Nevertheless, in general all simulations show a distinct response of the hydrology: For the ensemble forecast we found a decrease in snow and ice storage and earlier discharge and only slightly increased evapotranspiration sums, and an overall decrease in summer and autumn soil moisture. These results are completely in line with studies performed in the Swiss Alps by *Horton et al.* [2006] regarding discharge, *Etchevers et al.* [2002] and *Calanca* [2007] concerning evapotranspiration, and *Milner et al.* [2009] regarding snow and glaciers. We follow the argument of *Jasper et al.* [2004] that this accordance confirms our model outputs in general, and we plan to transfer these results to similar catchments.

[55] Few comparative studies have been reported regarding soil moisture and drought stress, but *Jasper et al.* [2004] showed evapotranspiration deficit dynamics similar to the Δ change dynamics we observed under different climate scenarios (Figure 5). In addition, *Jasper et al.* [2006] found similar soil moisture depletion at a much coarser scale and described the effects of altitude, slope, texture, and land use. In our study we found a major dependency on altitude and land use, the latter being likely due to changes in LAI and root depth. Based on a linear regression with altitude, the effect of elevation on soil moisture is not surprising. Further studies employing multiple hydrological models and different regionalization methods should be applied to derive catchment-specific patterns for the strongest responses to climate change. The combination of several models in a multimodel approach can further increase the reliability of a model result [*Schaefli*, 2005; *Breuer et al.*, 2009].

[56] A strong limitation to all the results presented in the present study is the assumption of a static vegetation cover. For sure, vegetation is very likely to change with a changing climate, especially in mountain areas. Furthermore, socioeconomic impacts and additional driving factors like fires might even more change the land cover in the Loetschen valley. In line with *Jasper et al.* [2004] we have to admit that our results are only one impact on the complex hydrological system. The consequences for soil moisture if trees germinated 500 m a.s.l. above the recent tree line or lay out pastures in formerly forested areas remain unclear. A sensitivity analysis under climate change scenario conditions might provide some insight in the future.

[57] Despite the good agreement of our results with those of other studies, there were some uncertainties originating from the hydrological model and the regionalization that were applied. The uncertainties in this study resulted from the applied models, the external input data, and the models' configuration and parameterization. Initially, uncertainty resulted from the simulation of soil moisture in this catchment at a high resolution. As shown in a previous study [*Rössler and Löffler*, 2010], this uncertainty in soil moisture simulation is primarily a consequence of the model's sensitivity to the skeleton fraction and the great spatial heterogeneity of soil properties in high mountain ecosystems [*Löffler*, 2005; *Löffler and Rössler*, 2005]. Further uncertainties originated from the hydrological model, as WaSiM-ETH uses a simple conceptual interflow approach (Schulla and Jasper, Model description WaSiM-ETH, 2007). This disadvantage should be kept in mind, particularly in high mountain areas presenting high relief complexity. A lack of interflow algorithms is not specific to WaSiM-ETH but is a general problem that arises from model algorithms and a lack of detailed data. A second source of uncertainty originated from model parameterization. As far as it was possible, all parameters were derived from field observations (e.g., vegetation height and root depth). Parameters that could not be derived were obtained from models with similar catchment characteristics [*Schulla*, 1997; *Verbunt et al.*, 2003] or suggested standard values (Schulla and Jasper, Model description WaSiM-ETH, 2007). Nevertheless, extended uncertainty analyses would increase confidence in the results of the hydrological model [*Saltelli et al.*, 2008]. The main second source of uncertainty originating from the downscaling approach and climate model was discussed previously.

[58] Despite these uncertainties, the impacts of climate change on soil moisture and drought stress are still relevant. Assuming that the uncertainties remain constant for reference and future scenario conditions, the change in soil moisture and drought stress indexes, such as WDS, must still be fully considered. Moreover, we found strongest soil moisture depletion and drought stress to occur in forested and nonforested areas below 1800 m a.s.l. As illustrated in Figure 3 (right) at this altitude the hydrological model tends to an overestimation of soil moisture. Hence "real" soil moisture depletion and drought stress might even be more sever.

[59] What are the consequences of increased drought stress? The predicted summer drought stress is likely to have severe effects on the ecosystem, especially on its vegetation. In a review, *Theurillat and Guisan* [2001] discussed the possible effects of summer drought stress on vegetation and confirmed this interpretation, but they also point out

that vegetation might adapt to altered climatic conditions. This adaptation cannot, of course, be simulated within the model. Nevertheless, *Allen et al.* [2010] also reviewed the actual impacts of recent climate change on forests worldwide and concluded that increased tree mortality due to climate change is already occurring. The first responses to recent heat waves, such as those in 2003, are currently observable in the decline of the pine forest in the neighboring Rhône valley as a result of drought stress and subsequent insect calamities [*Dobbertin et al.*, 2007]. Pine forests are found in the studied catchment up to 1500 m a.s.l. [*Hörsch*, 2001] and are therefore affected the most under future scenario conditions. Drought effects on forests represent a major threat to valley dwellers, as these forests are used for avalanche projection [*Brang et al.*, 2006].

6. Conclusion

[60] In conclusion, an ensemble forecast of future soil moisture was successfully conducted using two regional climate models that were downscaled using three different approaches in a mesoscale high mountain catchment at a high temporal and spatial resolution. Small differences in the variability of the downscaled data caused significant variability in daily drought stress. In the consensus of all models, soil moisture was found to decrease drastically in some areas, especially in areas already affected by drought stress. We found a major expansion of drought stress into the main valley under some model approaches, assuming static land covering. This expansion of water shortage will likely affect the growth of forests in the transition zones of dry and moist mountain ranges, whereas areas above 1800 m a.s.l. will remain nearly unaffected. Due to the high spatial resolution employed, the impact assessment of climatic change on soil moisture patterns can be easily utilized in forested and lower elevation areas, which adds considerable value to the findings of *Jasper et al.* [2006] at a coarser scale. In addition, the results from the ensemble forecast are not identical, but rather they offer a range of possibilities, as indicated by the ensemble variability. Thus, small changes in the setup of the model cause enormous deviations in the results.

[61] We found strong uncertainties related to the downscaling approach and the RCMs applied. Moreover, the choice of downscaling approach was found to be most relevant to the magnitude of depletion than the applied RCM, especially the representation of dry spells. *Jasper et al.* [2004] showed that uncertainties of simulated soil moisture depletion resulted from the variability of precipitation that originates from the choice of emission scenario and GCM in combination with the used regionalization method. Combining these two studies might lead to the conclusion that greatest uncertainty in soil moisture simulations under climate change is not related to the choice of method or climate model, but to the representation of precipitation and dry spells in specific. Recently developed model output statistics (MOS) as described by *Maraun et al.* [2010] might help to (1) correct the climate models, (2) downscale the RCMs appropriate, and (3) reproduce dry spells in a multisite framework of meteorological stations. But these MOS approaches need to be evaluated with hydrological models outputs to reduce artifacts that originate at the interface of hydrology und climatology.

[62] Over and above that, each of the three tested downscaling approaches Δ, DU, and SD present advantages and disadvantages, making the choice of a best downscaling method rather ambiguous. Nevertheless, the ensemble forecast of all six members is able to show a general trend in future hydrological responses to climate change: decreasing snow and ice storages, earlier discharge, only slightly increased evapotranspiration sums, and an overall decrease in summer and autumn soil moisture with strongest depletion and drought stress to occur in forested and nonforested areas below 1800 m a.s.l. Hence, multiple downscaling methods are needed and should be used in an ensemble forecast to address the uncertainties arising from the use of certain downscaling methods. These findings call into question the results of scenarios that are based on only a single downscaling approach.

[63] In conclusion, the results of this study, in conjunction with those of many published studies, indicate that uncertainties occur in each step involved in a climate change impact assessment, and it is only the magnitudes of these uncertainties that differ among studies. Hence, further studies should consider this finding by applying multimodel ensembles consisting of several emission scenarios, climate models, downscaling approaches, and several hydrological models.

[64] The idea of multimodel ensemble forecasting was recently applied to discharge in Ireland by *Bastola et al.* [2011] and produced remarkable results, with the hydrological model being the greatest source of uncertainty. The application of such a model to mountain soil moisture would be very useful. In addition, to address the multiple sources of uncertainties, the application of probabilistic forecasting, as suggested by *Araujo and New* [2007], might be an appropriate approach. However, this demands an enormous computational effort. Nevertheless, probabilistic forecasting might also be an interesting approach to communicate the uncertain results of such complex model approaches to local managers and decision makers, as it is much easier to work with probabilities than with ranges of possible values.

[65] **Acknowledgments.** The authors would like to thank to the German Research Foundation for financing this study (GRK437). Data were kindly provided by FOEN (discharge data), MeteoSwiss (meteorological station data), PRUDENCE (CHRM data), MPI Hamburg and UBA (REMO-UBA), GEOSTAT (soil and land use information), and U. Börst (GIUB, Bonn).

References

Allen, C. D., et al. (2010), A global overview of drought and heat-induced tree mortality reveals emerging climate change risks for forests, *For. Ecol. Manage.*, *259*, 660–684.

Araújo, M. B., and M. New (2007), Ensemble forecasting of species distributions, *Trends Ecol. Evol.*, *22*(1), 43–47.

Arnell, N. W., and N. S. Reynard (1996), The effects of climate change due to global warming on river flows in Great Britain, *J. Hydrol.*, *183*, 397–424.

Bastola, S., C. Murphy, and J. Sweeney (2011), The role of hydrological modelling uncertainties in climate change impact assessments of Irish river catchment, *Adv. Water Resourc.*, *34*, 562–576.

Bates, J. W., and C. W. Granger (1969), The combination of forecasts, *Oper. Res. Quat.*, *20*, 451–468.

Bavay, M., M. Lehning, T. Jonas, and H. Löwe (2009), Simulations of future snow cover and discharge in Alpine headwater catchments, *Hydrol. Processes*, *23*, 95–108.

Benestad, R. E. (2004), Empirical-statistical downscaling in climate modelling, *EOS*, *85*, 417–422.

Boden, A. G. (1994), *Bodenkundliche Kartieranleitung*, E. Schweizerbartsche, Hannover, Germany.
Börst, U. (2005), Nachhaltige Entwicklung im Hochgebirge. Eine Systemanalyse von Mensch-Umwelt-Szenarien im Lötschental (Zentral-Alpen), PhD Thesis, Uni Bonn, Bonn, http://hss.ulb.uni-bonn.de:90/2006/0710/0710-dt.htm, last access date 17 July 2011.
Bosshard, T., S. Kotlarski, T. Ewen, and C. Schär (2011), Spectral representation of the annual cycle in the climate change signal, *Hydrol. Earth Syst. Sci. Disc.*, *8*, 1161–1192.
Brang, P., W. Schönenberger, M. Frehner, R. Schwitter, J. J. Thormann, and B. Wasser (2006), Management of protection forests in the European Alps: An overview, *For. Snow Landscape Res.*, *80*, 23–44.
Breuer, L., et al. (2009), Assessing the impact of land use change on hydrology by ensemble modeling (LUCHEM). I: Model intercomparison with current land use, *Adv. Water Resourc.*, *32*, 129–146.
Brinkmann, W. A. R. (2002), Local versus REMOte grid points in climate downscaling, *Clim Res.*, *21*, 27–42.
Calanca, P. L. (2007), Climate change and drought occurrence in the Alpine region: How severe are becoming the extremes?, *Global Planet. Change*, *57*, 151–160.
Calanca, P. L., A. Roesch, K. Jasper, and M. Wild (2006), Global warming and the summertime evapotranspiration regime of the Alpine region, *Clim. Change*, *79*, 75–78.
Christensen, J. H., T. Carter, and F. Giorgi (2002), PRUDENCE employs new methods to assess European. Clim. Change, *EOS*, *83*, 147.
Christensen, N. S., and D. P. Lettenmaier (2007), A multimodel ensemble approach to assessment of climate change impacts on the hydrology and water resources of the Colorado River Basin, *Hydrol. Earth Syst. Sci.*, *11*, 1417–1434.
Davies, J. R., K. M. Lagueux, B. Sanderson, and T. J. Beechie (2007), Modeling stream channel characteristics from drainage-enforced dems in Puget sound, Washington, USA, *JAWRA*, *43*, 414–426.
Dibike, Y. D. and P. Coulibali (2006), Temporal neural networks for downscaling climate variability and extremes, *Neural Networks*, *19*, 135–144.
Dobbertin, M., B. Wermelinger, C. Bigler, M. Burgi, M. Carron, B. Forster, U. Gimmi, and A. Rigling (2007), Linking increasing drought stress to Scots pine mortality and bark beetle infestations, *Sci. World J.*, *7*, 231–239.
Dullinger, S., T. Dirnböck, and G. Grabherr (2004), Modelling climate change-driven treeline shifts: Relative effects of temperature increase, dispersal and invisibility, *J. Ecol.*, *92*, 241–252.
Eilers, J. (2000), Geomorphologie und Flächenbilanzierung im Lötschental, Diploma thesis. Department of Geography, Bonn.
Etchevers, P., C. Golaz, F. Habets, and J. Nolihan (2002), Impact of a climate change on the Rhone river catchment hydrology, *J. Geophys. Res.*, *107*(D16), 4293, doi:10.1029/2001JD000490.
Feddes, R. A., P. Kowail, K. Kolinska-Malinka, and H. Zaradny (1976), Simulation of field water uptake by plants using a soil water dependent root extraction function, *J. Hydrol. 31*, 13–26.
Finger, D., G. Heinrich, A. Gobiet, and A. Bauder (2012), Projections of future water resources and their uncertainty in a glacierized catchment in the Swiss Alps and the subsequent effects on hydropower production during the 21st century, *Water Resour. Res.*, *48*, W02521, doi:10.1029/2011WR010733.
Fischer, A. M., A. P. Weigel, C. M. Buser, R. Knutti, H. R. Künsch, M. A. Liniger, C. Schär, and C. Appenzeller (2012), Climate change projections for Switzerland based on a Bayesian multi-model approach, *J. Climatol.*, doi:10.1002/joc.3396, in press.
Fowler, H. J., S. Blenkinsop, and C. Tebaldi (2007), Linking climate change modelling to impacts studies: Recent advances in downscaling techniques for hydrological modeling, *J. Climatol.*, *27*, 1547–1578.
Frei, C., and C. Schär (1998), A precipitation climatology of the Alps from high-resolution rain-gauge observations, *J. Climatol.*, *18*, 873–900.
Frei, C., J. H. Christensen, M. Déqué, D. Jacob, R. G. Jones, and P. L. Vidale (2003), Daily precipitation statistics in regional climate models: Evaluation and intercomparison for the European Alps, *J. Geophys. Res.*, *108*(D3), 4124, doi:10.1029/2002JD002287.
Gellrich, M., P. Baur, B. Koch, and N. E. Zimmermann (2007), Agricultural land abandonment and natural forest re-growth in the Swiss mountains: A spatially explicit economic analysis, *Agric. Ecosyst. Environ.*, *118*, 93–108.
GEOSTAT (2000), *Digitale Bodeneignungskarte der Schweiz*, Swiss Federal Statistical Office, Bern.
GEOSTAT (2002), *Bodennutzung der Schweiz*, Source Arealstatistik 1992/1997, Swiss Federal Statistical Office, Bern.
Graham, L. P., J. Andreasson, and B. Carlsson (2007), Assessing climate change impacts on hydrology from an ensemble of regional climate models, model scales and linking methods—A case study on the Lule River basin, *Clim. Change*, *81*(Supplement), 293–307.
Green, W. H., and G. A. Ampt (1911), Studies on soil physics: I. The flow of air and water trough soils, *J. Agric. Sci.*, *4*, 1–24.
Gurtz, J., A. Baltensweiler, and H. Lang (1999), Spatially distributed hydrotope-based evapotranspiration and runoff in mountainous basins, *Hydrol. Processes*, *13*, 2751–2768.
Gurtz, J., M. Zappa, K. Jasper, H. Lang, M. Verbunt, A. Badoux, and T. Vitvar (2003), A comparative study in modelling runoff and its components in two mountainous catchments, *Hydrol. Processes*, *17*, 297–311.
Haylock, M. R., G. C. Cawley, C. Harpham, R. L. Wilby, and C. M. Goodess (2006), Downscaling heavy precipitation over the United Kingdom, a comparison of dynamical and statistical methods and their future scenarios, *Int. J. Climatol.*, *26*, 1397–1415.
Hewitson, B., and R. Crane (1996), Climate downscaling: Techniques and application, *Clim. Res.*, *7*, 85–95.
Hock, R. (1999), A distributed temperature-index ice- and snowmelt model including potential direct solar radiation, *J. Glaciol.*, *45*, 101–111.
Holsten, A., T. Vetter, K. Vohland, and V. Krysanova (2009), Impact of climate change on soil moisture dynamics in Brandenburg with a focus on nature conservation areas, *Ecol. Mod.*, *220*, 2076–2087.
Hörsch, B. (2001), Zusammenhang zwischen Vegetation und Relief in alpinen Einzugsgebieten des Wallis (Schweiz). PhD Thesis, University of Bonn, Bonn, 256. [Available at http://hss.ulb.uni-bonn.de:90/2001/0168/0168.htm], last access date 17 July 2011.
Horton, P., B. Schaefli, A. Mezghani, B. Hingray, and A. Musy (2006), Assessment of climate-change impacts on alpine discharge regimes with climate model uncertainty, *Hydrol. Processes*, *20*, 2091–2109.
Huss, M., D. Farinotti, A. Bauder, and M. Funk (2008), Modelling runoff from highly glacierized alpine drainage basins in a changing climate, *Hydrol. Processes*, *22*, 3888–3902.
IPCC (2007), *Clim. Change 2007: The Physical Science Basis*, Contribution of Working Group I to the Fourth Assessment Report of the Intergovernmental Panel on Clim. Change, edited by S. Solomon et al., Cambridge Univ Press, Cambridge.
Jacob, D. (2001), A note to the simulation of the annual and inter-annual variability of the water budget over the Baltic Sea drainage basin, *Meteorol. Atmos. Phys.*, *77*, 61–73.
Jasper, K., P. L. Calanca, D. Gyalistras, and J. Fuhrer (2004), Differential impacts of climate change on the hydrology of two alpine river basins, *Clim. Res.*, *26*, 113–129.
Jasper, K., P. Calanca, and J. Fuhrer (2006), Changes in summertime soil water patterns in complex terrain due to climatic change, *J. Hydrol.*, *327*, 550–563.
Khan, M. S., and P. Coulibaly (2010), Assessing hydrologic impact of climate change with uncertainty estimates: Bayesian neural network approach, *J. Hydrometeorol.*, *11*, 482–495.
Khan, M. S., P. Coulibaly, and Y. Dibike (2006), Uncertainty analysis of statistical downscaling methods, *J. Hydrol.*, *319*, 357–382.
Köhn, M. (1928), Bemerkungen zur mechanischen Bodenanalyse, III Ein neuer Pipettapparat, *Z. Pflanzenernährung, Düngung, Bodenkunde*, *11*, 50–54.
Köplin, N., D. Viviroli, B. Schädler, and R. Weingartner (2010), How does climate change affect mesoscale catchments in Switzerland? A framework for a comprehensive assessment, *Adv. Geosci.*, *27*, 111–119.
Körner, C. (2003), *Alpine Plant Life*, Springer, Berlin.
Kunstmann, H., K. Schneider, R. Forkel, and R. Knoche (2004), Impact analysis of climate change for an Alpine catchment using high resolution dynamic downscaling of ECHAM4 time slices, *Hydrol. Earth Syst. Sci.*, *8*, 1030–1044.
Lenderink, G., A. Buishand, and W. van Deursen (2007), Estimates of future discharge of the river Rhine using two scenario methodologies: Direct versus delta approach, *Hydrol. Earth Syst. Sci.*, *11*, 1145–1159.
Löffler, J. (2005), Snow cover dynamics, soil moisture variability, and vegetation ecology in high mountain catchments of central Norway, *Hydrol. Processes*, *19*, 2385–2405.
Löffler, J., and O. Rössler (2005), Climatologic and hydrologic coupling in the ecology of Norwegian high mountain catchments, in *Climate and Hydrology in Mountain Areas*, edited by C. deJong et al., pp. 195–224, Wiley, Chichester, UK.
Lüthi, D., A. Cress, H. C. Davies, C. Frei, and C. Schär (1996), Interannual variability and regional climate simulations, *Theor. Appl. Climatol.*, *53*, 185–209.
Maraun, D. et al. (2010), Precipitation downscaling under climate change. Recent developments to bridge the gap between dynamical models and the end user, *Rev. Geophys.*, *48*, RG3003, doi:10.1029/2009RG000314.

Martinec, J. (1975), Snowmelt runoff model for river flow forecasts, *Nord. Hydrol.*, *6*, 145–154.

Matera, A., G. Fontana, and V. Marletto (2007), Use of a new agricultural drought index within a regional drought observatory, in *Methods and Tools for Drought Analysis and Management*, edited by G. Rossi, pp. 103–124, Springer, Dordrecht, Netherlands.

Middelkoop, H., K. Daamen, D. Gellens, W. Grabs, J. C. J. Kwadijk, H. Lang, B. W. A. H. Parmet, B. Schädler, J. Schulla, and K. Wilke (2001), Impact of climate change on hydrological regimes and water resources management in the Rhine basin, *Clim. Change*, *49*, 105–128.

Milner, A. M., L. E. Brown, and D. M. Hannah (2009), Hydroecological response of river systems to shrinking glaciers, *Hydrol. Processes*, *23*, 62–77.

Monteith, J. L. (1975), *Vegetation and the Atmosphere, Vol. 1: Principles*, Academic, London.

Naden, P. S., and C. D. Watts (2001), Estimating climate-induced change in soil moisture at the landscape scale: An application to five areas of ecological interest in the U.K., *Clim. Change*, *49*(4), 411–440.

Narasimhan, B., and R. Srinivasan (2005), Development and evaluation of soil moisture deficit index (SMDI) and evapotranspiration deficit index (ETDI) for agricultural drought monitoring, *Agric. For. Meteorol.*, *133*, 69–88.

Nash, J. E., and J. V. Sutcliffe (1970), River flow forecasting through conceptual models. Part I—A discussion of principles, *J. Hydrol.*, *10*, 282–290.

Paul, F., M. Maisch, C. Rothenbühler, M. Hoelzle, and W. Haeberli (2007), Calculation and visualisation of future glacier extent in the Swiss Alps by means of hypsographic modelling, *Global Planet Change*, *55*, 343–357.

Paul, F., A. Linsbauer, and W. Haeberli (2011), Grossräumige Modellierung von Schwundszenarien für alle Schweizer Gletscher, Klimaänderung und Wasserkraft, Sektorielle Studie Wallis, Modul B Gletscherszenarien, Technical report, WWK-Schlussbericht des Geographischen Instituts der Universität Zürich (GIUZ). Source: http://www.geo.uzh.ch/~alinsbau/publ/berichte/Klimaaenderung_und_Wasserkraft_Gletscherszenarien_GIUZ.pdf, Geographisches Institut Universität Zürich, Zürich Schweiz.

Poesen, J., and H. Lavee (1994), Rock fragments in top soils: Significance and processes, *Catena*, *23*, 1–28.

Prudhomme, C., N. Reynard, and S. Crooks (2002), Downscaling of global climate models for flood frequency analysis: where are we now?, *Hydrol. Processes*, *16*, 1137–1150.

Räisänen, J., U. Hansson, A. Ullerstig, R. Döscher, L. P. Graham, C. Jones, H. E. M. Meier, P. Samuelson, and U. Willén (2004), European climate in the late twenty-first century: Regional simulations with two driving global models and two forcing scenarios, *Clim. Dyn.*, *22*, 13–31.

Rawls, W. J., and D. L. Brakensiek (1985), Prediction of soil water properties for hydrologic modeling, in *Watershed Manage*, edited by E. Jones E, and T. J. Ward, pp. 293–299, ASCE, New York.

Rebetez, M., and M. Dobbertin (2004), Climate change may already threaten Scots pine stands in the Swiss Alps, *Theor. Appl. Climatol.*, *79*(1–2), 1–9.

Rodriguez-Iturbe, I. (2000), Ecohydrology: A hydrologic perspective of climate-soil-vegetation dynamics, *Water Resour. Res.*, *36*(1), 3–9.

Rössler, O., and J. Löffler (2010), Potentials and limitations of modelling spatio-temporal patterns of soil moisture in a high mountain catchment using WaSiM-ETH, *Hydrol. Processes*, *24*(15), 2182–2196.

Saltelli, A., M. Ratto, T. Andres, F. Campolongo, J. Cariboni, and D. Gatelli (2008), *Global sensitivity analysis: The Primer*, John Wiley, New York.

Schaefli, B. (2005), Quantification of modelling uncertainties in climate change impact studies on water resources: Application to a glacier-fed hydropower production system in the Swiss Alps, Dissertation, EPFL, Lausanne, Switzerland. [Available at http://library.epfl.ch/en/theses/?nr=3225.]

Schär, C., P. L. Vidale, D. Lüthi, C. Frei, C. Häberli, M. A. Liniger, and C. Appenzeller (2004), The role of increasing temperature variability in European summer heatwaves, *Nature*, *427*, 332–336.

Schmidt, S., B. Weber, and M. Winiger (2009), Analyses of seasonal snow disappearance in an alpine valley from micro- to meso-scale (Loetschental, Switzerland), *Hydrol. Processes*, *23*, 1041–1051.

Schneebeli, M., and P. Bebi (2004), Snow and avalanche control, in *Encyclopedia of Forest Sciences*, edited by J. Burley et al., pp. 397–4012, Elsevier, New York.

Schulla, J. (1997), Hydrologische Modellierung von Flussgebieten zur Abschätzung der Folgen von Klimaänderungen, Dissertation, 161 pp., Zürcher Geographische Schriften, Zürich.

Segui, P. Q., A. Ribes, E. Martin, F. Habets, and J. Boé (2010), Comparison of three downscaling methods in simulating the impact of climate change on the hydrology of Mediterranean basins, *J. Hydrol.*, *383*, 111–124.

Shinohara, Y., T. Kumagai, K. Otsuki, A. Kume, and N. Wada (2009), Impact of climate change on runoff from a mid-latitude mountainous catchment in central Japan, *Hydrol. Processes*, *23*, 1418–1429.

Sivakumar, M. V. K., R. P. Motha, D. A. Wilhite, and D. A. Wood (2011), Agricultural Drought Indices, Proceedings of the WMO/UNISDR Expert Group Meeting on Agricultural Drought Indices, 2–4 June 2010, *AGM-11, WMO/TD No. 1572; WAOB-2011*, 197 pp., World Meteorological Organization, Murcia, Spain, Geneva, Switzerland.

Stott, P. A., and C. E. Forest (2007), Ensemble climate predictions using climate models and observational constraints, *Philos. Trans. R. Soc.*, *365*, 2029–2052.

SWISSTOPO (2004), *Das digitale Höhenmodell der Schweiz 1: 25000*, Federal Office of Topography, Wabern.

Teich, M., and P. Bebi (2009), Evaluating the benefit of avalanche protection forest with GIS-based risk analyses—A case study in Switzerland, *For. Ecol. Manage.*, *257*, 1910–1919.

Themessl, M. J., A. Gobiet, and A. Leuprecht (2011), Empirical-statistical downscaling and error correction of daily precipitation from regional climate models, *J. Climatol.*, *31*, 1530–1544.

Theurillat, J. P., and A. Guisan (2001), Potential impact of climate change on vegetation in the European Alps: A review, *Clim. Change*, *50*(1–2), 77–109.

van Genuchten, M. T. (1980), A closed-form equation for predicting the hydraulic conductivity of unsaturated soils, *Soil Sci. Soc. Am. J.*, *44*, 892–898.

Verbunt, M., J. Gurtz, K. Jasper, H. Lang, P. Warmerdam, and M. Zappa (2003), The hydrological role of snow and glaciers in alpine river basins and their distributed modeling, *J. Hydrol.*, *282*, 36–55.

Vidale, P. L., D. Lüthi, C. Frei, S. Seneviratne, and C. Schär (2003), Predictability and uncertainty in a regional climate model, *J. Geophys. Res.*, *108*(D18), 4586, doi:10.1029/2002JD002810.

Viney, N. R. et al. (2009), Assessing the impact of land use change on hydrology by ensemble modelling (LUCHEM) II: Ensemble combinations and predictions, *Adv. Water Res.*, *32*, 147–158.

Viviroli, D. et al. (2011), Climate change and mountain water resources: Overview and recommendations for research, management and policy, *Hydrol. Earth Syst. Sci.*, *15*, 471–504.

Welpmann, M. (1997), Geomorphologie und Naturgefahren im Lötschental (Schweiz), Diploma Thesis, Department of Geography, Bonn.

Welpmann, M. (2003), Bodentemperaturmessungen und simulationen im Lötschental, PhD Thesis, University of Bonn, Bonn, 256. [Available at http://hss.ulb.uni-bonn.de/2003/0290/0290.htm], last access date: 10 December 2011.

Wilby, R. L., and I. Harris (2006), A framework for assessing uncertainties in climate change impacts: Low-flow scenarios for the River Thames, UK, *Water Resour. Res.*, *42*, W02419, doi:10.1029/2005WR004065.

Wilby, R. L., and T. M. L. Wigley (1997), Downscaling general circulation model output: A review of methods and limitations, *Progress Phys. Geogr. 21*, 530–548.

Wilby, R. L., C. W. Dawson, and E. M. Barrow (2001), SDSM—A decision support tool for the assessment of regional climate change impacts, *Environ. Model. Software*, *17*, 145–157.

Wilby, R. L., O. J. Tomlinson, and C. W. Dawson (2003), Multi-site simulation of precipitation by conditional resampling, *Clim. Res.*, *23*, 183–194.

Willmott, C. J. (1981), On the validation of models, *Phys. Geogr.*, *1*, 184–194.

Wood, A. W., L. R. Leung, V. Sridhar, and D. P. Lettenmaier (2004), Hydrologic implications of dynamical and statistical approaches to downscaling climate model outputs, *Clim. Change*, *62*, 189–216.

Xu, C. Y. (1999), From GCMs to river flow: A review of downscaling methods and hydrologic modelling approaches, *Progress Phys. Geogr.*, *23*, 229–249.

Yang, Y., M. Watanabe, Z. Wang, Y. Sakura, and C. Tang (2009), Prediction of changes in soil moisture associated with climatic changes and their implications for vegetation changes: Waves model simulation on Taihang mountain, China, *Clim. Change*, *57*, 163–183.

Zargar, A., R. Sadiq, B. Naser, and F. I. Khan (2011), A review of drought indices, *Environ. Rev.*, *19*, 333–349.

Zierl, B., and H. Bugmann (2005), Global change impacts on hydrological processes in Alpine catchments, *Water Resour. Res.*, *41*, W02028, doi:10.1029/2004WR003447.

B. Diekkrüger and J. Löffler, Department of Geography, University of Bonn, Meckenheimer Allee 166, 53115 Bonn, Germany.

O. Rössler, Oeschger Centre for Climate Change Research, Institute of Geography, Group of Hydrology, Hallerstrasse 12, 3012 Bern, Switzerland. (ole.roessler@giub.unibe.ch)